Roles for Rice Membrane Dynamics and Plasmodesmata during Biotrophic Invasion by the Blast Fungus [W][OA]

Prasanna Kankanala,[a] Kirk Czymmek,[b] and Barbara Valent[a],[1]

[a] Department of Plant Pathology, Kansas State University, Manhattan, Kansas 66506
[b] Delaware Biotechnology Institute, University of Delaware, Newark, Delaware 19711

Rice blast disease is caused by the hemibiotrophic fungus *Magnaporthe oryzae*, which invades living plant cells using intracellular invasive hyphae (IH) that grow from one cell to the next. The cellular and molecular processes by which this occurs are not understood. We applied live-cell imaging to characterize the spatial and temporal development of IH and plant responses inside successively invaded rice (*Oryza sativa*) cells. Loading experiments with the endocytotic tracker FM4-64 showed dynamic plant membranes around IH. IH were sealed in a plant membrane, termed the extra-invasive hyphal membrane (EIHM), which showed multiple connections to peripheral rice cell membranes. The IH switched between pseudohyphal and filamentous growth. Successive cell invasions were biotrophic, although each invaded cell appeared to have lost viability when the fungus moved into adjacent cells. EIHM formed distinct membrane caps at the tips of IH that initially grew in neighboring cells. Time-lapse imaging showed IH scanning plant cell walls before crossing, and transmission electron microscopy showed IH preferentially contacting or crossing cell walls at pit fields. This and additional evidence strongly suggest that IH co-opt plasmodesmata for cell-to-cell movement. Analysis of biotrophic blast invasion will significantly contribute to our understanding of normal plant processes and allow the characterization of secreted fungal effectors that affect these processes.

INTRODUCTION

The hemibiotrophic ascomyceteous fungus *Magnaporthe oryzae*, which belongs to the *Magnaporthe grisea* species complex (Couch and Kohn, 2002), includes the devastating rice blast pathogen on rice (*Oryza sativa*) (Kawasaki, 2004) as well as economically important pathogens on wheat (*Triticum aestivum*) (Urashima et al., 2004) and other cereals and grasses (Farman, 2002; Zellerhoff et al., 2006). The blast fungus mechanically breaches the outer plant surface using an appressorium, a dome-shaped cell that generates enormous turgor pressure (Howard and Valent, 1996; Talbot, 2003). The appressorium produces a specialized hypha, a penetration peg, which pierces the plant surface. The cytoplasm of a penetration peg initially contains abundant actin microfilaments and lacks recognizable cytoplasmic organelles, including ribosomes (Bourett and Howard, 1992). Upon reaching the epidermal cell lumen, the penetration peg expands to form a narrow filamentous primary hypha. The peg then becomes a conduit for moving the nucleus and cytoplasmic contents from the appressorium into the growing primary hypha. In the compatible interaction, primary hyphae differentiate into thicker, bulbous invasive hyphae (IH) that fill the first-invaded cells and then move into neighboring cells (Heath et al., 1990). Extensive cytological studies of blast disease have shown that the initial plant cell invasions are biotrophic, because invaded cells appear healthy and retain the ability to plasmolyze (Koga et al., 2004, and references therein). During a major resistance (*R*) gene–mediated incompatible interaction, invaded plant cells lose membrane integrity and the ability to plasmolyze and show cytoplasmic granulation and autofluorescence (Koga and Horino, 1984a; Peng and Shishiyama, 1989; Koga, 1994b; Koga et al., 2004). Understanding the mechanisms by which blast IH invade living rice cells is critical for understanding disease mechanisms as well as the mechanisms of *R* gene–mediated resistance that rice breeders manipulate in attempts to control this disease (Jia et al., 2004; Kawasaki, 2004).

Few genes that affect biotrophic growth of the blast fungus have been identified, because extensive mutational analyses have mainly identified genes with a role in appressorium structure and function (Talbot, 2003). As in bacterial pathosystems (Desveaux et al., 2006), blast effector genes that are likely to be secreted inside living host cells have been identified by their avirulence activity in conferring recognition and resistance mediated by major rice *R* genes (Kawasaki, 2004). A few *R* genes and avirulence (*AVR*) genes have been cloned (Sweigard et al., 1995; Farman et al., 2002; Böhnert et al., 2004; Qu et al., 2006), and in one case, the rice *R* gene *Pi-ta* and its corresponding *AVR-Pita* gene from the fungus were cloned and their interaction characterized (Bryan et al., 2000; Orbach et al., 2000). AVR-Pita protein appears to interact directly with Pi-ta, and transient expression of this avirulence/effector protein in the cytoplasm of rice cells with Pi-ta triggers hypersensitive resistance (Jia et al., 2000). This suggests that the fungus delivers AVR-Pita protein into the cytoplasm of the rice cell. Although AVR-Pita appears to function as a protease inside rice cells, its role in the invasion process is not yet understood. To understand how AVR-Pita and

other blast effectors function in promoting rice blast disease, it is first necessary to understand how the fungus co-opts normal plant cell processes for successful colonization of host tissue.

Understanding the nature of the interface between blast IH and rice is critical for future studies to understand how pathogen effectors are secreted inside plant cells. The current literature contains contradictory reports on the nature of the IH–plant cytoplasm interface in rice blast disease. One report presented experimental evidence suggesting that IH were separated from host cytoplasm by invaginated plasma membrane (PM), and another report presented evidence suggesting that blast IH breached the plant PM and grew directly within the rice cytoplasm (Koga and Horino, 1984b; Heath et al., 1992). Biotrophic hyphae produced by other fungi and oomycetes, including (hemi)biotrophic pathogens and arbuscular mycorrhizal symbionts, are embedded in the plant cytoplasm but remain separated from the cytoplasm by invaginated PM (Heath and Skalamera, 1996; Mendgen and Hahn, 2002; Harrison, 2005; O'Connell and Panstruga, 2006). The biotroph–plant cell interface is relatively well studied for fungi such as rusts that grow intercellularly and produce terminal feeding structures called haustoria inside living plant cells. Haustoria are surrounded by an interfacial extrahaustorial matrix between the fungal cell wall and the extrahaustorial membrane (EHM). For dikaryotic rusts and powdery mildews, annular neckband structures attach the plant PM to the haustorial neck and produce a specialized matrix compartment that is separate from the plant apoplast (O'Connell and Panstruga, 2006). In contrast with biotrophic haustorial fungi, hemibiotrophic Colletotrichum species produce biotrophic IH that either lack an interfacial matix (Latunde-Dada, 2001; Wharton et al., 2001; O'Connell et al., 2004) or contain a simplified matrix without a neckband (O'Connell et al., 1985; O'Connell and Panstruga, 2006). Transmission electron microscopy (TEM) analyses showed that the interfacial matrix is generally amorphous and uniform in appearance, although the molecular composition of interfacial matrices appears to vary in different pathosystems (Stark-Urnau and Mendgen, 1995; O'Connell and Panstruga, 2006).

In contrast with biotrophic hyphae, necrotrophic hyphae are associated with the death of plant cells ahead of the fungal growth front, and they lack a specialized interface in the plant cell. This is best illustrated for the hemibiotrophic pathogens in Colletotrichum species, which undergo two-stage infection cycles that begin with intracellular biotrophic hyphae and then switch to necrotrophic hyphae (Latunde-Dada, 2001; Wharton et al., 2001; O'Connell et al., 2004). Colletotrichum species initially undergo cell invasion by biotrophic intracellular infection vesicles and enlarged biotrophic primary hyphae, both of which invaginate the host PM. Depending on the Colletotrichum species investigated, biotrophic invasion involves one or a few plant cells. Then, biotrophic primary hyphae differentiate into narrow, filamentous secondary hyphae that lack invaginated PM and kill host cells before invasion. Necrotrophic hyphae are typically thinner and grow in the host cell walls or in the lumens of dead host cells. Unlike biotrophic hyphae, necrotrophic hyphae do not constrict when they cross the host cell wall. Additionally, host walls show signs of enzymatic digestion in the presence of necrotrophic hyphae. Mutational analyses support the occurrence of distinct biotrophic and necrotrophic phases for Colleto-

trichum species, because pathogen genes have been identified that have a role in switching from biotrophy to necrotrophy (Latunde-Dada, 2001; O'Connell et al., 2004). By contrast, distinct biotrophic and necrotrophic phases have not been documented for the blast fungus, and despite extensive screening for nonpathogenic mutants in M. oryzae, no genes that block the predicted switch have been discovered (Talbot, 2003).

There are increasing reports of interactions occurring at the biotroph–plant cytoplasm interface. For example, TEM with high-pressure frozen and freeze-substituted (HPF/FS) samples provided excellent detail in the interfacial region for the downy mildew Hyaloperonospora parasitica on leaves of Arabidopsis thaliana (Mims et al., 2004). The extrahaustorial matrix and EHM were highly irregular in outline, and numerous vesicles appeared to either fuse with or bleb off the EHM. Another TEM study provided evidence that plant endocytosis occurred at the biotroph–plant interface based on immunolocalization of clathrin on tubular coated pits in the EHM surrounding haustoria of the monokaryotic cowpea (Vigna unguiculata) rust Uromyces vignae (Stark-Urnau and Mendgen, 1995). Koh et al. (2005) used live-cell confocal microscopy to study the powdery mildew fungus Erysiphe cichoracearum in epidermal cells of Arabidopsis. They used Arabidopsis plants engineered to tag various organelles with green fluorescent protein (GFP) and reported very active plant PM dynamics, both near and distal to the penetration site. In an interesting example of a pathogen preparing its host cell before invasion, Koh et al. (2005) report that the epidermal PM showed invaginations underneath developing appressoria before penetration occurred. Haustoria subsequently grew into these membrane pouches. A dramatic case of a fungus controlling plant cell processes before entering the plant cell has been reported for a symbiotic arbuscular mycorrhizal fungus on Medicago truncatula (Genre et al., 2005). To reach the root cortex and form intracellular arbuscules (analogous to haustoria), the fungus produces an appressorium that controls host nuclear movement, cytoskeletal elements, and endoplasmic reticulum to build a prepenetration apparatus inside root epidermal cells. This elaborate structure appears to be involved in building an apoplastic compartment that the fungus uses to cross the epidermal cell. These examples illustrate the way that biotrophic hyphae co-opt normal plant cell processes and thus suggest potential functions for biotrophic effectors that are secreted inside the plant cell (O'Connell and Panstruga, 2006).

Mechanisms used by biotrophic fungi, including the blast fungus, for moving from one cell to the next are not understood, although there are reports that this process involves localized cell wall degradation and mechanical pressure (Heath et al., 1992; Xu and Mendgen, 1997; Martinez et al., 1999). Among plant pathogens known to move from one living cell to another, only viruses have been studied extensively. Viruses manipulate plasmodesmata for their cell-to-cell movement (Lazarowitz and Beachy, 1999; Zambryski and Crawford, 2000). Plasmodesmata are the PM-lined channels that cross plant cell walls and connect the cytoplasms of plant cells into a symplastic network. Plasmodesmata contain appressed endoplasmic reticulum (the desmotubule), proteins, and cytoskeletal elements. These components define a cytoplasmic sleeve through plasmodesmata that allows the passage of small molecules and some proteins. Viruses

produce movement proteins (MPs) that increase the size exclusion limit of plasmodesmata without noticeable structural changes (Zambryski and Crawford, 2000). MPs act as molecular chaperones and assist single-stranded viral nucleic acids to move through plasmodesmata. For some viruses, the movement of intact virions or subviral particles through plasmodesmata is associated with the production of tubules ～50 nm in diameter that extend out from the plant cell wall (Ward et al., 1997; Lazarowitz and Beachy, 1999). Mechanisms that biotrophic intracellular hyphae use to move from cell to cell must take into account the much larger diameter of these hyphae relative to viruses that spread through plasmodesmata.

In this study, we investigated the nature of the fungus–plant interface and cell-to-cell invasion in the fully susceptible interaction characteristic of rice blast disease in the field. We studied biotrophic blast invasion using live-cell fluorescence and confocal microscopy with fluorescent probes that identify particular plant and fungal components. This microscopic analysis involved >950 independent infection sites using four different fluorescent probes. Key results were confirmed using TEM with HPF/FS samples, which provided improved preservation of membranes compared with conventional chemical fixation methods (Bourett et al., 1999; Mims et al., 2004). We documented an amazing degree of plasticity in the intracellular biotrophic IH responsible for rice blast disease. We demonstrated that the differentiation of primary hyphae into bulbous IH included an event that sealed IH inside a tightly fitted plant-derived extra-invasive hyphal membrane (EIHM), which prevented apoplastically applied FM4-64 from reaching the fungal PM. Bulbous IH exhibited pseudohyphal growth and searched for locations to cross cell walls into neighboring cells. At certain locations, IH swelled and crossed the wall using highly constricted IH pegs that became primary hyphae-like filamentous IH inside the next cell. The filamentous IH enlarged into bulbous IH, and this biotrophic invasion process was repeated in successive rice cells. EIHM encasing filamentous IH had distinctive membrane caps that were not seen on bulbous IH. Blast IH lacked a uniform interfacial matrix, although rare patches of complex plant cellular components occurred between the EIHM and IH wall. Plant membrane dynamics were dramatically affected in the vicinity of the fungus. We present evidence suggesting that IH use plasmodesmata for moving into the next live cell. This would require IH to constrict at least 100-fold to approach the diameter of a plasmodesma (～30 to 50 nm) (Cook et al., 1997). Understanding the cellular strategies used for biotrophic plant cell invasion in a pathosystem in which genetic analysis and genome resources are available for both the fungus (Dean et al., 2005) and rice (International Rice Genome Sequencing Project, 2005) will allow the elucidation of plant cellular mechanisms as well as mechanisms critical for this important fungus–plant interaction.

RESULTS

Intracellular IH, but Not Primary Hyphae, Are Sealed within Host Membrane

We produced a fungal strain, KV1, with constitutive, cytoplasmic expression of enhanced yellow fluorescent protein (EYFP) and visualized its invasion of rice leaf sheath epidermal cells. This rice

tissue is optically clear and relatively flat, which facilitates live-cell imaging (Koga et al., 2004). To assess whether major *R* gene–mediated specificity is maintained in leaf sheaths under our assay conditions, we compared compatible and incompatible interactions mediated by the *Pi-ta* resistance gene. KV1, which expresses avirulence gene *AVR-Pita*, is compatible with rice variety YT16 (*pi-ta⁻*) and incompatible with rice variety Yashiro-mochi (*Pi-ta*). We assayed the ability of invaded plant cells to plasmolyze as an indicator of membrane integrity and cell viability (Koga et al., 2004; O'Connell et al., 2004). As expected from other studies (Koga and Horino, 1984a; Koga et al., 2004), KV1-invaded host cells of susceptible YT16 plasmolyzed at 27 h post inoculation (hpi), and most invaded host cells (98%) of resistant Yashiro-mochi failed to plasmolyze at this same stage of invasion (Table 1). Retention of *Pi-ta* mediated resistance specificity in infected leaf sheath pieces suggested that cellular studies of disease development in this system will be relevant to leaf cell invasion, which is responsible for much devastation in the field.

Our approach to understanding detailed cell biological events in the compatible interaction was to first investigate whether IH were surrounded by rice membrane inside the first-invaded epidermal cell. Membranes surrounding haustoria in other pathogen systems lacked normal plant PM proteins because they failed to label with chimeric, fluorescent PM proteins (Koh et al., 2005; O'Connell and Panstruga, 2006). Considering the possibility of such failure, we first attempted to label plant PM in infected rice sheath cells with the membrane-selective dyes hexyl-rhodamine B (RB) and FM4-64. The RB dye is passively taken up by cells and integrated into all internal membranes, including the endoplasmic reticulum. FM4-64 inserts in PM and diffuses laterally into contiguous membranes. The dye moves into internal cellular membranes only through an active, time-dependent endocytotic process, finally reaching vacuolar membranes. In other plants, FM4-64 failed to label the endoplasmic reticulum and nuclear membranes (Bolte et al., 2004). In the rice sheath cells, RB labeled the lace-like network characteristic of endoplasmic reticulum and FM4-64 did not (Figures 1A and 1B). Both FM4-64 and RB staining showed membrane aggregation near the site of appressorial penetration (Figures 1A and 1B), as has been documented previously in other host–pathogen systems (O'Connell and Panstruga, 2006). The diffuse staining pattern of RB around and inside IH sharply contrasted with the FM4-64 fluorescence closely outlining the IH. Therefore, endoplasmic reticulum and other rice cell membranes aggregated around IH but remained outside a tightly fitting, FM4-64–labeled membrane surrounding IH.

Table 1. Viability of Rice Cells Invaded by the *AVR-Pita*–Containing Rice Pathogen KV1 in Compatible and Incompatible Interactions

Rice Variety	Plasmolysis	No Plasmolysis
YT-16 (*pi-ta*)	120 (100%)	0
Yashiro-mochi (*Pi-ta*)	2 (100%)	98

Values shown are numbers of first-invaded epidermal cells (at 27 hpi) that plasmolyzed in 0.75 M sucrose. For all rice cells that plasmolyzed, the percentage of cells in which the IH were included within the shrinking protoplast is shown in parentheses.
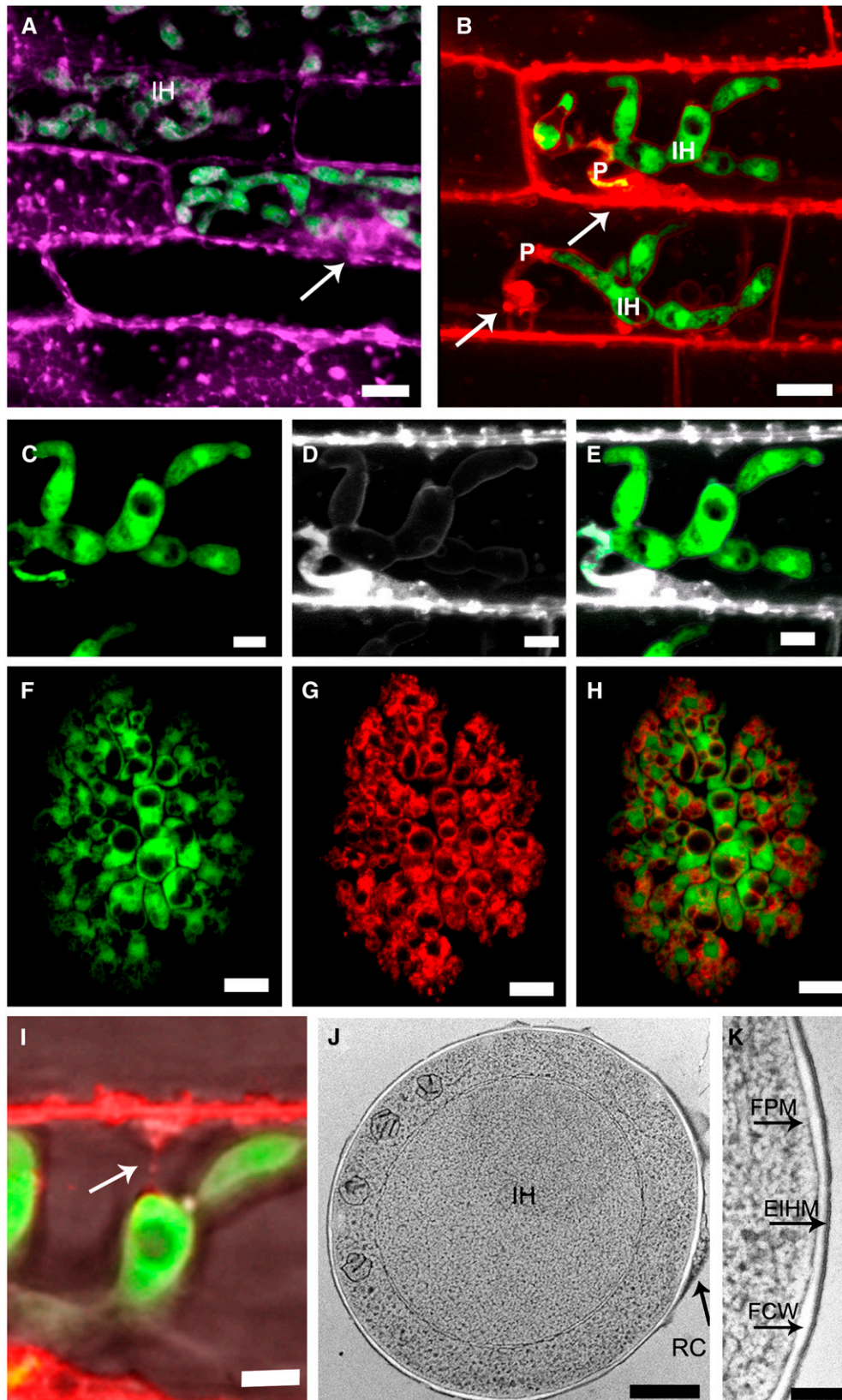
Figure 1. Live-Cell Imaging of *M. oryzae* IH and Rice Cell Membranes.

We recorded confocal images of 80 FM4-64–stained sheath epidermal cells with IH developing at 27 hpi. These images reflect the expected dimorphism of thin, filamentous primary hyphae and bulbous IH (Figures 1B to 1E). Alternative fates of the primary hyphae are illustrated in two contiguous cells in Figure 1B. The primary hypha in the upper rice cell showed colocalization of EYFP and FM4-64 fluorescence (yellow area) and was presumed alive. The primary hypha in the lower rice cell lacked EYFP fluorescence and was apparently dead. At this time, primary hyphae lack EYFP expression in 50% ($n = 80$) of the infection sites surveyed. This suggested that primary hyphae were dispensable once IH were established inside the rice cell.

Both primary hyphae and IH internalized the endoplasmic reticulum dye RB (data not shown). However, there was a major difference in the FM4-64 staining patterns for these two hyphal types. Whereas living primary hyphae (expressing EYFP) were brightly fluorescent as a result of internal FM4-64 staining, IH were closely outlined by a thin layer of FM4-64 fluorescence and lacked internal FM4-64 fluorescence. This is clearly illustrated by separation of the EYFP and FM4-64 channels (Figures 1C to 1E) for the upper sheath cell in Figure 1B. The lack of internal FM4-64 fluorescence inside IH was especially obvious in the IH septal and vacuolar membranes, which were expected to accumulate the dye (Atkinson et al., 2002). Thus, primary hyphae internalized FM4-64 but IH did not.

One explanation for the failure of IH to internalize FM4-64 would be that they were enveloped by a plant membrane that prevented the dye from reaching the fungal PM. Alternatively, IH inside the rice cell may lack endocytotic capabilities. In support of the first explanation, the septal PM of IH never labeled with FM4-64. One would predict that if FM4-64 inserted in the fungal PM, it would label septal PM by lateral diffusion without the need for endocytosis (Atkinson et al., 2002). In addition, several lines of evidence make the latter alternative unlikely: (1) spores and germ tubes of the fungus on the plant surface internalize FM4-64 by endocytosis (Atkinson et al., 2002; our unpublished results); (2) rare IH inside susceptible rice tissues had internalized FM4-64, showing that at least some IH were capable of taking up the dye (in these cases, IH with internal FM4-64 staining showed diminished EYFP fluorescence, suggesting that they were unhealthy or dying); and (3) invasive-like hyphae formed in dialysis mem-

branes (Bourett and Howard, 1990) internalized FM4-64 within 20 min, confirming that similar hyphae formed in vitro undergo endocytosis (Figures 1F to 1H). Together, these results suggested that healthy IH inside plant cells were sealed within a plant membrane that blocked the access of fungal membranes to FM4-64 uptake. We named this plant membrane the EIHM. FM4-64 staining showed connections between the EIHM and rice membranes across the cell (Figure 1I).

To confirm the presence of EIHM surrounding IH, we performed TEM with similarly infected sheath samples prepared by HPF/FS. The TEM images confirmed that IH were encased in a membrane outside the fungal cell wall (Figures 1J and 1K). Together, our results settled a long-standing question (Koga and Horino, 1984b; Heath et al., 1992) by demonstrating that IH were tightly encased in host membrane as they grew within host epidermal cells.

Enhanced Rice Membrane Dynamics in Cells with IH

FM4-64 is generally used as an endocytosis marker during early stages of loading the dye (Bolte et al., 2004). We performed experiments to visualize the time course of dye uptake in infected sheath epidermal cells. Apparently because of the sheath cuticle, the time course of dye incorporation is not uniform for all plant cells. Epidermal cells near stomata and cells near some appressoria were the first to internalize the dye. Therefore, the time course of dye uptake in a particular cell depends on the location of that cell relative to points of dye entry across the plant cuticle.

We visualized FM4-64 uptake in individual cells at early stages before internal plant cellular membranes were loaded with dye by identifying epidermal cells in which neither the EIHM nor the entire PM was stained. In the example shown in Figures 2A and 2B, only portions of the PM were stained with the dye (see Supplemental Movies 1 and 2 online). In addition, at this early stage, the dye had not yet loaded into internal rice membranes. Confocal imaging showed that numerous FM4-64–labeled membrane tubules extended from the labeled PM toward IH. Figure 2A and Supplemental Movie 1 online show a membrane tubule that was separate from the plant PM. After 4 min, this tubule appeared to be rounding up, as if forming a round vesicle (Figure 2B; see Supplemental Movie 2 online). Tubular and round vesicles were abundant in cells with IH but not in uninvaded cells. Based on their

Figure 1. (continued).

(A) and **(B)** Differential staining patterns with RB and FM4-64 in rice sheath epidermal cells invaded by EYFP-labeled fungal strain KV1 (green). Arrows indicate sites where appressoria had penetrated into host cells.

(A) RB dye (purple) stained the endoplasmic reticulum inside rice cells and fungal IH at 36 hpi. Bar = 10 μm.

(B) PM and endocytotic membranes in rice cells were stained to saturation with FM4-64 (red). Narrow primary hyphae (P) extending from the penetration site differentiated into bulbous IH inside two invaded rice cells at 27 hpi. This image is a three-dimensional projection of 20 optical sections acquired with a z-interval of 0.44 μm. Bar = 10 μm.

(C) to **(E)** FM4-64 outlines IH but is not internalized by them. These images show separate and merged fluorescence channels for the upper rice cell in Figure 1B. Shown are EYFP fluorescence **(C)**, FM4-64 fluorescence (white in this image) **(D)**, and merged channels **(E)**. Bars = 5 μm.

(F) to **(H)** Invasive-like hyphae formed in vitro on dialysis membrane internalize FM4-64. Shown are EYFP fluorescence **(F)**, FM4-64 fluorescence (red) **(G)**, and merged channels **(H)**. Bars = 10 μm.

(I) The membrane encasing the IH had an FM4-64–stained connection (arrow) to rice membrane at the cell periphery. This is an enlarged view of a single optical section from the infection site in **(C)** to **(E)**. The bright-field channel is included in this view (gray scale). Bar = 5 μm.

(J) and **(K)** TEM images show EIHM surrounding an IH inside an epidermal cell.

(J) Transverse section of an IH at 26 hpi. The arrow indicates a fibrillar inclusion inside the generally close-fitting EIHM. RC, rice cell. Bar = 500 nm.

(K) High-magnification view of the IH–host interface from the cell in **(J)**. FCW, fungal cell wall; FPM, fungal plasma membrane. Bar = 150 nm.
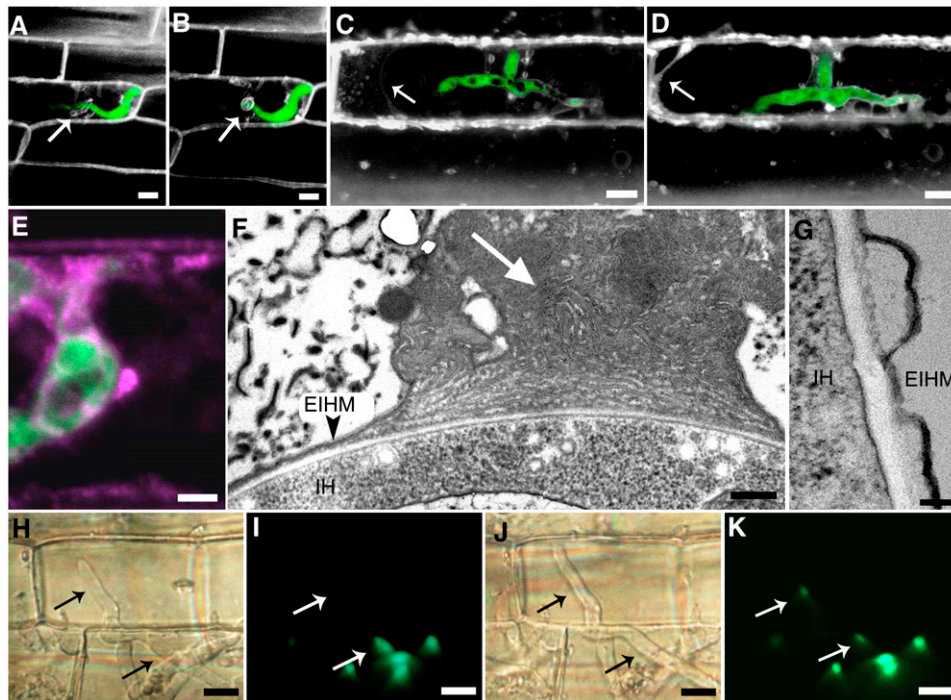
Figure 2. Rice Membrane Dynamics and Fungal Nuclear Movement.

(A) and **(B)** Numerous membrane tubules occur around an IH (green) in an epidermal cell during early stages of FM4-64 (white) uptake. Arrows indicate a membrane tubule **(A)** that appeared to be rounding up 4 min later **(B)**. Note that **(A)** is imaged at a slightly lower magnification than **(B)**. Each image is a projection of four optical sections taken at 0.5-μm z-intervals. Complete z-series are shown in Supplemental Movies 1 and 2 online. Bars = 10 μm.

(C) and **(D)** Shifting of internal rice membranes (white) around an IH (green) after loading to saturation with FM4-64. Arrows indicate a shift in the rice vacuolar membrane position from **(C)** to **(D)** 90 min later. Numerous connections are seen between the EIHM and peripheral rice membranes. Both images are projections of four optical sections taken at 0.5-μm z-intervals. Complete z-series are shown in Supplemental Movies 3 and 4 online. Bars = 10 μm.

(E) Endoplasmic reticulum (purple) in an RB-stained epidermal cell aggregated around the IH (green) at 36 hpi. Bar = 5 μm.

(F) TEM image of a complex aggregation (white arrow) of endoplasmic reticulum–like membrane and vesicles internalized between the EIHM (black arrowhead) and the IH cell wall. Bar = 150 nm.

(G) TEM image of EIHM elaborations containing electron-transparent material between the membrane and the IH wall. Bar = 75 nm.

(H) to **(K)** Fungal nuclear movement to IH growing in neighboring cells. Infected cells were visualized using differential interference contrast (DIC) optics (**[H]** and **[J]**). IH nuclei were visualized by fluorescence from a histone-GFP fusion protein expressed by the fungus (**[I]** and **[K]**). Ten minutes elapsed between **(H)/(I)** and **(J)/(K)**. Arrows mark equivalent cellular positions for the localization of nuclear fluorescence relative to the developing IH. The lower arrows indicate fading nuclear fluorescence in **(K)** relative to **(I)**, and the upper arrows indicate the appearance of nuclear fluorescence in **(K)** relative to **(I)**. Bars = 10 μm.

FM4-64 staining characteristics, these vesicles appeared to be endocytotic compartments derived from the rice PM. These early-stage FM4-64 internalization studies showed enhanced vesicular activity in the vicinity of the fungus.

Microscopy of infected cells that were saturated with FM4-64 showed the dynamic nature of other host membranes around the growing IH. At this later stage of dye loading, internal rice membranes, including vacuolar membranes, were stained. Images of an infected cell taken 90 min apart showed different membrane connections between the EIHM and peripheral rice membranes (Figures 2C and 2D; see Supplemental Movies 3 and 4 online). Membranes in the rice cell moved to surround the IH during this time period, as shown in the Supplemental Movies online. The position of the vacuole also appeared to have shifted, as indicated by arrows in Figures 2C and 2D. The FM4-64 patterns were distinct from the diffuse RB patterns showing endoplasmic reticulum surrounding IH (Figure 2E). This comparison confirmed that host endoplasmic reticulum surrounded the developing IH but generally remained outside the EIHM.

TEM analysis showed that the EIHM was generally closely appressed to the fungal cell wall, with no apparent matrix material separating the plant membrane from the fungal wall (Figure 1J). However, the EIHM sometimes exhibited irregular localized elaborations, and some of these elaborations contained fibrillar (Figures 1J and 2F), electron-transparent (Figure 2G), or electron-opaque (data not shown) material inside. In two independent examples, the EIHM appeared to enclose extensive cellular components, including endoplasmic reticulum–like membranes inside the EIHM and in direct contact with the fungal cell wall (Figure 2F). We conclude that blast IH lack a defined, uniform

interfacial matrix between the IH wall and the EIHM. However, diverse cellular materials were sometimes incorporated inside this interfacial zone.

Biotrophic Invasion Continues in Neighboring Rice Cells

The IH in the second- and later-invaded rice cells differed in behavior, and often in appearance, from the IH in the first-invaded cell. After penetrating the host cell at 24 hpi, IH grew in the first-invaded cell for 8 to 12 h, often filling it up. A time-dependent switch occurred during this period, because IH tended to spread into neighboring cells between 32 and 36 hpi no matter how quickly, or how completely, the first cell had been filled with fungus. The initial hyphae that formed after internal cell wall penetrations were thin and filamentous (filamentous IH) compared with the bulbous IH in the first-invaded cell (Table 2). The filamentous IH enlarged into IH that we will continue to refer to as bulbous IH, although they generally appeared less bulbous than IH in first-invaded cells. Bulbous IH in subsequently invaded cells grew more rapidly from one cell to the next, requiring only 2 to 3 h to move into neighboring cells.

Fungal strains that expressed a histone-GFP fusion protein for labeling nuclei initially showed no nuclear fluorescence within IH growing in neighboring cells (Figures 2H to 2K). Apparently, IH could show significant growth before a nucleus moved from IH in the previous rice cell. Filamentous IH in neighboring cells were seen to thicken up, branch, and undergo pseudohyphae-like budding (see Supplemental Movie 5 online). A similar phenomenon was observed early in the infection process when primary hyphae penetrated into the first-invaded host cell (data not shown). Primary hyphae were thin and anucleate. Nuclei entered primary hyphae around the time that they differentiated into IH.

We assessed the biotrophic invasion of successively invaded cells using a plasmolysis assay. Compatible rice cells containing IH plasmolyzed at 27 hpi, suggesting that the cell's PM was intact and functional at this time (Figure 3A, Table 1). These first-invaded plant cells failed to plasmolyze after 32 hpi, indicating that the PM was no longer intact. This finding suggested that a host cell was no longer viable by the time the fungus exited it. Neighboring rice cells that were penetrated, even by multiple hyphae, were initially able to undergo plasmolysis (Figure 3B). The plasmolyzing protoplast always shrank around the IH ($n > 125$) and did not retract along the hyphae from their site of entry into the cell (Figures 3A and 3B, Table 1). This is consistent with FM4-64 labeling studies in suggesting the fungus was sealed inside the plant PM.

To quantify the level of plasmolysis during successive cell invasions, we observed the ability to plasmolyze in the first-, the second-, and the third- or fourth-invaded plant cells. In this analysis, we focused on plant cells containing IH that had not yet exited the cell. Seventy percent to 90% ($n > 110$ at each time point) of these invaded plant cells plasmolyzed (Figure 3C). Cells that failed to plasmolyze had generally reached the late cell colonization stage just before the fungus moved on into neighboring cells. These results were consistent with our previous finding that plant cells no longer plasmolyzed around the time the fungus moved into the next cell. Plasmolysis patterns observed in this study were consistent with our previous observations (Table 1) that IH were always enclosed within the shrinking protoplast. Together, the plasmolysis experiments indicated that the blast fungus sequentially invaded living rice cells.

FM4-64 uptake studies showed that IH growing in neighboring cells were sheathed in EIHM. An unusual feature of the EIHM surrounding the filamentous IH that had just entered neighboring rice cells was the prominent dome-shaped cap at the hyphal tips (Figures 3D and 3E, Table 2). The caps were clearly visible with DIC microscopy before these IH had grown halfway across the cell (Figure 3D). FM4-64 loading studies confirmed that the caps represented EIHM that extended ahead of the hyphal tips (Figure 3E). Three-dimensional optical sectioning of the entire cell in Figure 3D showed six filamentous IH invading neighbors, including the three shown. All six had membrane caps. Similarly, the IH in Figure 3E had produced 12 filamentous IH, including the 5 shown. All 12 had membrane caps. We used laser scanning confocal microscopy to examine filamentous IH from seven additional cells. In total, membrane caps were visible for 45 of 50 filamentous IH (90%) that had grown less than halfway across the second cell. Membrane caps were also seen at the tips of the filamentous primary hyphae inside first-invaded cells (data not shown). However, differentiated bulbous IH uniformly lacked membrane caps. Therefore, membrane caps were a structural feature of the plant membrane surrounding primary hyphae and filamentous IH before they differentiated into bulbous IH.

As with the bulbous IH in first-invaded cells, IH in second-, third-, and fourth-invaded plant cells failed to internalize FM4-64. We

Table 2. Comparison of Blast Hyphal Types Involved in Biotrophic Invasion of Rice

Biological Features	Primary Hypha	Bulbous IH	Filamentous IH
Growth style	Filamentous	Pseudohyphal and filamentous	Filamentous
Hyphal diameter	3 to 5 μm	>5 μm	3 to 5 μm
Differentiates from	Appressorial penetration peg	Primary hypha or filamentous IH	IH peg that crosses internal walls
Internalizes FM4-64	Yes	No	No
Has membrane cap	Yes	No	Yes
Viability maintained during lesion formation	No	Yes	Yes

Primary hyphae differentiate into bulbous IH as described by Heath et al. (1990). Bulbous IH include the pseudohyphal forms in the first-invaded cell and the enlarged filamentous to pseudohyphal forms in subsequently invaded cells. Filamentous IH are the thin transient hyphae that grow in cells directly after crossing of internal walls.
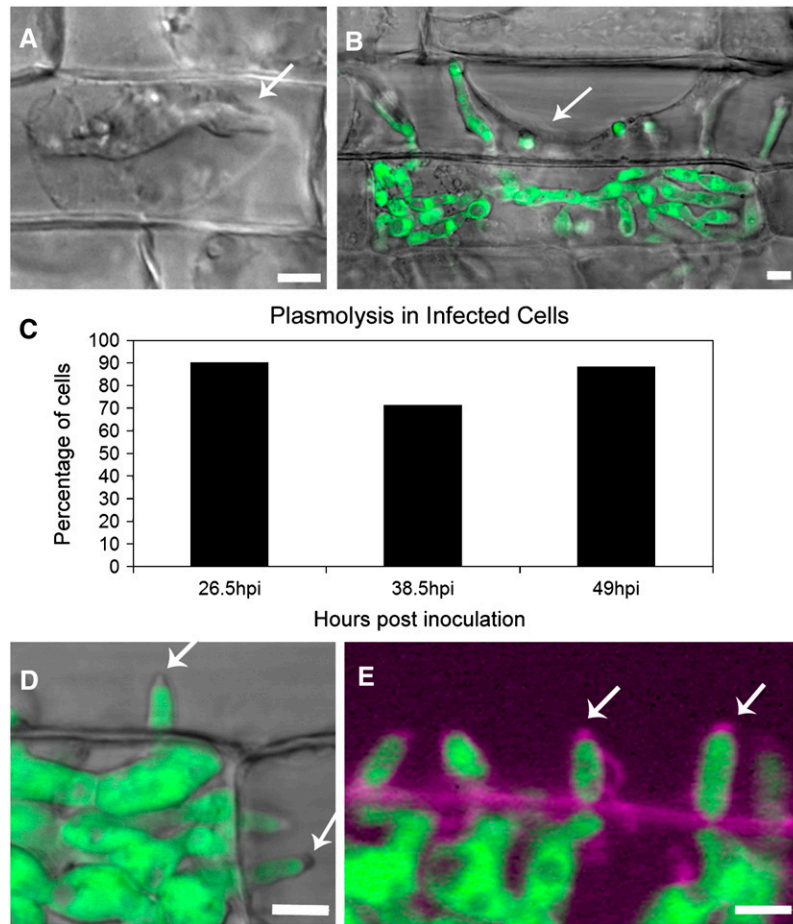
Figure 3. Biotrophic Invasion Continues in Neighboring Rice Cells.

(A) An IH was surrounded by the shrinking protoplast (arrow) after plasmolysis in 0.75 M sucrose solution. These cells were visualized at 27 hpi using DIC optics. Bar = 5 μm.

(B) A rice cell at 48 hpi still plasmolyzes even though seven IH have invaded it from the first-invaded cell. This image shows the green hyphal fluorescence merged with the bright field (gray scale) of the plasmolyzed plant PM (arrow). Note that all IH expressed strong EYFP fluorescence. Some IH in this view do not appear green because they were below the focal plane. Bar = 5 μm.

(C) Quantification of plasmolysis in successively invaded rice cells. Percentage of plasmolysis was measured in first-invaded cells at 26.5 hpi, in second-invaded cells at 38.5 hpi, and in third- or fourth-invaded cells at 49 hpi. This experiment was performed independently from the experiment in Table 1.

(D) and **(E)** Filamentous IH growing in rice epidermal cells were sheathed in EIHM with prominent membrane caps at their tips (arrows). The membrane caps visible by DIC microscopy **(D)** stained with FM4-64 dye, shown as purple **(E)**. Bars = 5 μm.

conclude that these hyphae are also enveloped by plant membrane that blocks dye from reaching fungal membranes. Therefore, filamentous and bulbous IH inside neighboring plant cells were biotrophic. During this study, we did not observe rice cell death ahead of the fungus, nor did we observe fungus growing into nonplasmolyzing cells. Our results are consistent with an extended biotrophic invasion strategy in rice blast disease.

IH Appear to Exploit Plasmodesmata for Cell-to-Cell Movement

Time-lapse confocal imaging (Figures 4A to 4D; see Supplemental Movie 5 online) demonstrated that the IH often exhibit

budding, pseudohyphae-like growth instead of typical filamentous tip growth (Gancedo, 2001). IH appeared to search for specific locations to cross the plant cell wall. This sometimes took the form of a hyphal tip repeatedly touching the wall and moving away (arrowheads in Figures 4A to 4D; see Supplemental Movie 5 online). Often, hyphae that reached the cell wall grew along it for a period before crossing. Two IH that had traveled for at least 5 μm along the wall before crossing are indicated (stars in Figures 4A to 4D). Finally, some IH grew along the wall for extended periods without crossing, suggesting that they had not found favorable conditions to cross. These results suggested that the fungus sought out specific locations to cross the plant cell wall.

At certain locations, IH stopped scanning and swelled slightly before sending a highly constricted hypha across the wall (arrows in Figures 4A to 4D). These constricted hyphae developed from apically expanding IH in a similar manner to the development of penetration pegs from appressoria. Therefore, we refer to these specialized hyphae as IH pegs. The IH peg expanded and grew as filamentous IH in the new cell. Although it had previously been reported that IH constrict when they move across walls (Czymmek et al., 2002; Rodrigues et al., 2003), live-cell imaging showed the extreme degree of this constriction (Figure 4E; see Supplemental Figure 1 online). Because of this level of constriction and the searching behavior of IH, we hy-

pothesized that they sought out plasmodesmata, which are clustered in pit field regions of the wall (Zambryski and Crawford, 2000).

To investigate potential associations between IH and plasmodesmata, we performed ultrastructural analysis on infected rice sheath cells. IH and plasmodesmata in sheath tissues were visualized using TEM with HPF/FS samples. Approximately 25 invaded cells were sampled in one study of infected tissue at 36 hpi. Twelve of these cells contained IH that had either touched or moved across the host cell wall. We used semithick (250 nm) tissue sections to observe any fine connections between IH and the rice cell walls. Plasmodesmata were seen at 9 of 10 locations
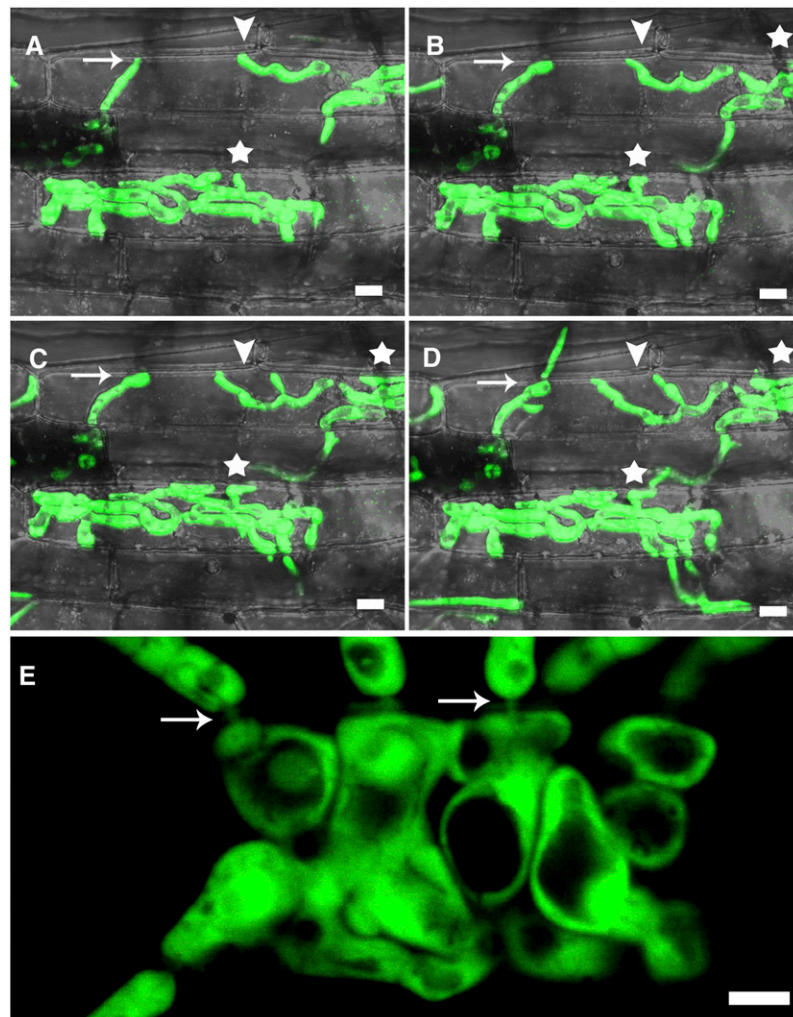
Figure 4. Live-Cell Imaging Suggested That Cell-to-Cell Movement Involves Plasmodesmata.

(A) to **(D)** IH seek out specific locations to cross rice cell walls. Four still images from Supplemental Movie 5 online show IH growing in epidermal cells. Image **(A)** was obtained at 36 hpi. During the 2.5-h period recorded, an IH (arrow) reached the cell wall and swelled slightly before crossing. The arrowhead indicates a fixed point in the cell and shows an IH developing by pseudohyphal budding and moving over time. Stars indicate IH that had each moved along the rice cell wall for ~5 μm before swelling and crossing. The IH in the top right corner was not visible in **(A)**. Other examples can be seen in the movie, in addition to IH growing along the cell wall and not crossing. Bars = 5 μm.
(E) IH at 32 hpi exhibit extreme constriction (arrows) as they cross the rice cell wall. Only EYFP fluorescence is shown. This same image with merged EYFP and FM4-64 channels (see Supplemental Figure 1 online) indicates the locations of rice cell walls. Bar = 5 μm.

in which the fungus had direct physical contact with the wall. For example, a section that just grazed the tip of an IH showed fine interconnections between the IH and a pit field (Figure 5A). Another IH showed fine interconnections with the plant wall at a pit field (Figure 5B). In this view, a few interconnections were seen outside the visible pit field where the IH was farther away from the wall. Yet another IH was closely pressed against the cell wall at a pit field region (Figure 5C). We failed to see plasmodesmata at only 1 of the 10 contact locations in this analysis. Therefore, this TEM analysis of infected tissue at 36 hpi, and similar results from infected tissue at 48 hpi (data not shown), showed that close associations between IH and the plant cell wall generally occurred at pit fields.

The TEM analysis of infected tissue at 36 hpi showed two events in which an IH had crossed the cell wall. In both cases, IH had crossed the cell wall adjacent to a normal-appearing plasmodesma (Figure 5D). These micrographs strongly suggested that blast IH crossed the plant cell wall at pit fields. The IH crossing the wall was ~10-fold larger in diameter than the plasmodesmatal channel beside it. The region in the cell wall traversed by the IH appeared well defined, without signs of mechanical or enzymatic damage.

Guard cells lack functional plasmodesmata (Zambryski and Crawford, 2000; Oparka and Roberts, 2001). If the fungus uses functional plasmodesmata to cross the plant cell wall, it should not be able to move into guard cells. To test this prediction, we visualized IH at later infection stages (48 to 72 hpi) to ensure that the fungus had ample time and opportunity to grow into guard cells. Fungus failed to enter guard cells at 98 of 100 infection sites in which it had heavily colonized the surrounding cells. At the two remaining sites, a browning response made it difficult to determine whether there was fungus inside the guard cells. Figure 6A illustrates how IH can tightly pack a subsidiary cell without moving into the guard cell. These results are consistent with the hypothesis that the fungus uses functional plasmodesmata to cross the plant cell wall.

We attempted to colocalize a plasmodesmata-specific fluorescent protein with IH crossing the wall. We performed transient plant expression assays with particle bombardment transformation in attempts to express GFP-labeled tobacco mosaic virus movement protein (TMV-MP) (Oparka et al., 1997) in rice cells with growing IH. Fluorescently labeled TMV-MP labeled punctae characteristic of plasmodesmata in transformed rice leaf sheath cells, but it failed to move into neighboring rice cells. In five independent experiments, we failed to observe epidermal cells that contained both IH and fluorescent TMV-MP. We did observe IH growing in rice cells undergoing transient expression of cytoplasmic GFP, suggesting that wounding as a result of microprojectile bombardment was not inhibiting the growth of the fungus in the transformed cells.
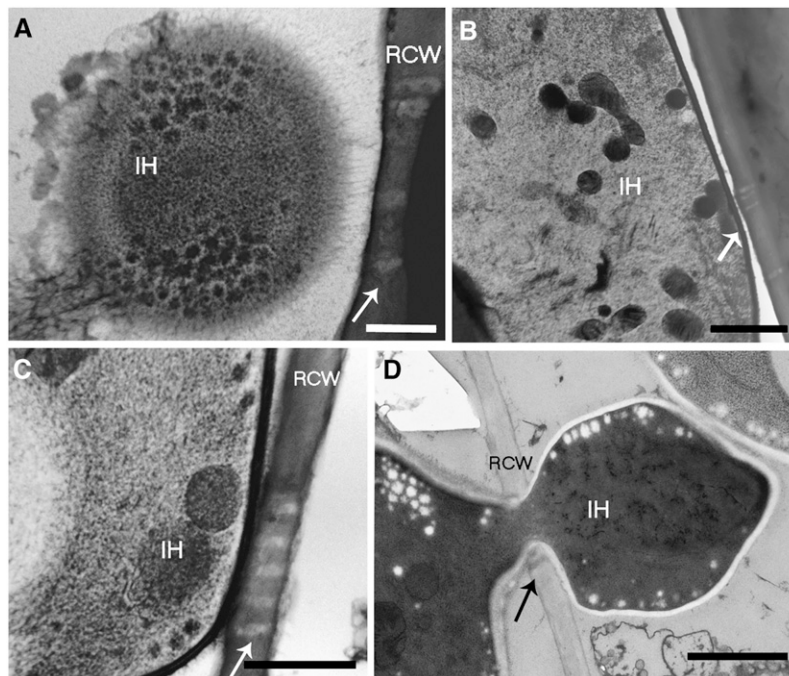

Figure 5. TEM Images Show IH Associated with Plasmodesmata.

(A) to **(C)** IH associated with rice cell walls (RCW) at pit fields. Arrows indicate plasmodesmata. Semithick sections (250 nm) were used to visualize fine connections between IH and pit fields. Therefore, the resolution of individual plasmodesma was reduced.
(A) and **(B)** Two views of IH with fibrillar extensions toward pit fields. Note that the section just grazed the tip of the hypha in **(A)**. Bars = 300 nm in **(A)** and 800 nm in **(B)**.
(C) An IH pressed against the cell wall at a pit field. Bar = 500 nm.
(D) Ultrathin section (80 nm) of an IH that had traversed the host cell wall beside a plasmodesma (arrow). Bar = 1 μm.
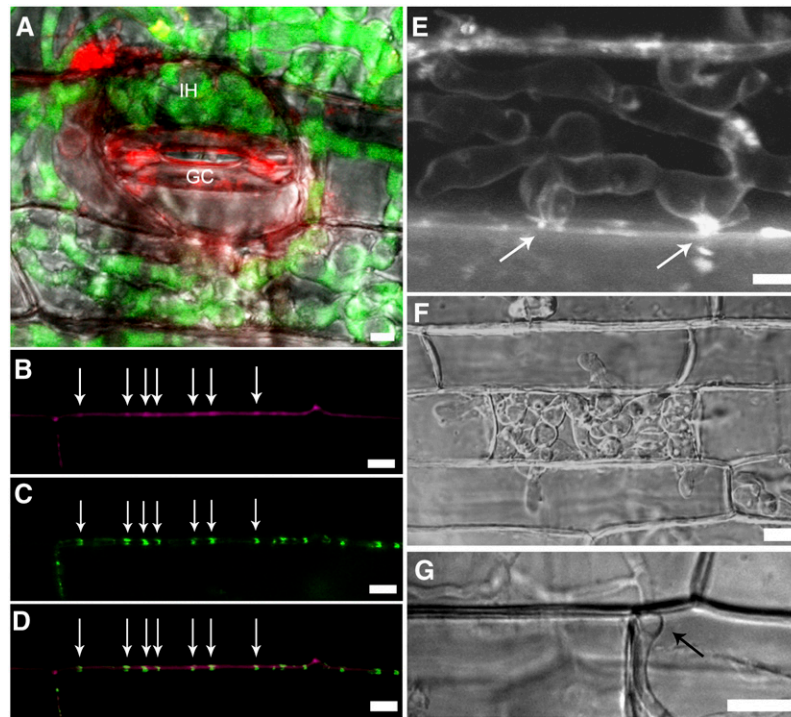
Figure 6. Images Relating to Plasmodesmata and Cell-to-Cell Movement.

(A) IH (green) packed into a subsidiary cell failed to invade the neighboring guard cell. Plant membranes were stained with FM4-64 at 48 hpi. This image is a projection of 10 optical sections, each 1 μm thick. GC, guard cell. Bar = 5 μm.

(B) to **(D)** Colocalization of GFP-labeled TMV-MP and FM4-64 spots identify pit fields (arrows) in epidermal walls. Shown are FM4-64 fluorescence (purple) **(B)**, MP-GFP fluorescence (green) **(C)**, and merged channels **(D)**. Bars = 10 μm.

(E) FM4-64 staining (white) of an IH at 36 hpi showed EIHM that appeared continuous with the membranes in pit field regions. EYFP and bright-field channels are not shown to highlight the FM4-64 pattern. The left arrow indicates an IH with two adjacent membrane connections, and the right arrow indicates an example in which the EIHM appeared continuous with membrane in the adjacent cell. Bar = 5 μm.

(F) and **(G)** An *alb⁻* mutant that fails to produce the high pressure needed for appressorial penetration crosses internal walls normally. DIC images show infection at 38 hpi **(F)** and 42 hpi **(G)**. The arrow indicates swelling before movement. Bars = 10 μm.

Transient expression assays with the fluorescent TMV-MP confirmed that brighter fluorescent spots in plant cell walls stained with FM4-64 corresponded to pit fields. We predicted this because PMs of adjacent cells are continuous through plasmodesmata. The fluorescence of the TMV-MP colocalized with these FM4-64 punctae (Figures 6B to 6D). Several other examples of the FM4-64 staining pattern in the cell walls can be seen in Supplemental Movies 1 to 4 online. In confocal studies of FM4-64–stained tissues, we documented examples in which the EIHM had connections with pit fields. This is illustrated by an image of a late-stage IH (36 hpi) that had filled the first-invaded rice cell (Figure 6E). Only the FM4-64 fluorescence is shown to highlight the EIHM around the IH and other plant membranes. Note that this apparently healthy IH was expressing EYFP (data not shown) and that it had not internalized FM4-64. For the left hypha contacting the plant wall in Figure 6E, the EIHM had two connections that tethered the IH to FM4-64–stained spots at the wall. For the IH contacting the plant wall at the right (Figure 6E), the EIHM was continuous with FM4-64–stained membranes that appeared to cross the wall into the next cell. Plasmodesmata are the only known locations where membranes, both PM and endo-plasmic reticulum, cross from one plant cell to the next. Therefore, this confocal image associates IH with plasmodesmata.

Together, the searching behavior of IH, the extreme constriction of IH crossing the wall, the TEM experiments that showed that the fungus contacts the cell wall preferentially at pit fields, and TEM images of IH moving across the wall at pit fields strongly suggested that the fungus uses plasmodesmata for its cell-to-cell movement. This hypothesis is also supported by the failure of IH to enter guard cells and by additional confocal imaging of the EIHM connections to FM4-64–labeled regions in the host cell wall.

## Crossing Internal Plant Walls Does Not Require High Turgor Pressure

Some aspects of the biology of the hyphal pegs used by IH to cross internal plant cell walls appeared similar to the biology of penetration pegs produced by appressoria to cross the plant cuticle and outer epidermal wall (Howard and Valent, 1996). In both cases, apically expanding (swollen) hyphal cells produce highly constricted hyphae that cross the wall. These constricted hyphae expand into thin filamentous hyphae that grow for a short

period before differentiating into bulbous IH (Table 2). We have shown that in both cases, the thin hyphae that grow immediately after wall crossings have distinctive membrane caps (Figures 3D and 3E; data not shown).

Appressoria produce and focus high turgor pressures to force penetration pegs through the outer plant surface (Howard and Valent, 1996). To test whether high turgor pressure might be involved in crossing internal plant walls, we observed tissue colonization by a melanin biosynthesis mutant incapable of building high pressure. The *alb−* mutant CP721, which is defective in the polyketide synthase responsible for the first step in melanin biosynthesis (Howard and Valent, 1996), was inoculated onto lightly wounded inner leaf sheath tissue. The mutant produced unmelanized appressoria on the abraded sheath cuticle, some of which penetrated into epidermal cells. The mutant produced IH that colonized the first-invaded host cell and then moved into neighboring cells in a manner indistinguishable from the wild type (Figure 6F). Furthermore, the mutant still exhibited characteristic swelling before crossing internal cell walls (Figure 6G). We conclude that, although the fungus may require some pressure produced by the swollen fungal cells to cross internal plant cell walls, it does not require the extremely high melanin-derived turgor pressures required by appressoria to pierce the outer plant surface.

Later Infection Stages and Leaf Colonization

To determine whether the health of the fungus was maintained in the initially invaded cells as later cells were filling with fungus, we checked for EYFP expression and for propidium iodide uptake (Figure 7). Propidium iodide is internalized only in fungal hyphae with damaged membranes. Very few fungal hyphae in developing lesions stained red as a result of the uptake of propidium iodide. The rarity of the colocalization of propidium iodide and EYFP fluorescence confirmed that cells that were taking up propidium iodide had generally lost EYFP expression and presumably were not viable. This image shows the variation in shapes of bulbous IH
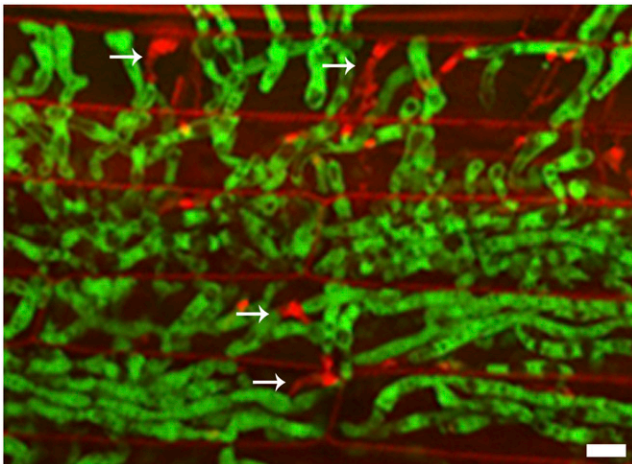
Figure 7. Viability and Morphology of IH in Invaded Rice Sheath Cells.

Propidium iodide staining (red) identifies dead IH (arrows) among EYFP-expressing IH (green) in infected leaf sheath cells at 55 hpi. Bar = 10 µm.

in planta. The IH continued to swell and constrict during the crossing of normal-appearing plant cell walls. Unlike primary hyphae in the first-invaded cells, filamentous IH maintained viability as the lesion developed. This produced an interconnected hyphal network that showed high levels of EYFP expression by IH throughout the colonized tissue, even though the only actively growing IH were at lesion margins. Sporulation began in the first-invaded cells days after they filled with IH.

We determined whether the biotrophic invasion strategy we described in the leaf sheath assay occurred in rice leaves. The easiest feature of biotrophic invasion to visualize in green leaves was the swelling of the IH and hyphal constriction through the plant cell walls. Extensive fungal growth was seen in rice leaf tissue at 72 hpi (see Supplemental Figure 2 online). A higher magnification confocal image of a densely invaded area of the leaf showed extensive hyphal swelling and constriction (see Supplemental Figure 2 online). In a related study of leaf infection, Berruyer et al. (2006) reported that the fungal growth front always preceded symptom development even at later stages of leaf colonization. Together, these results suggested that the blast fungus uses an extended biotrophic invasion strategy in leaves as well as in leaf sheaths.

DISCUSSION

Rice Membrane Dynamics and Biotrophic Blast Invasion

This analysis of biotrophic rice blast invasion has revealed new features of cellular mechanisms resulting in disease. We have characterized three distinct types of hyphae (Table 2) that play a role in biotrophic invasion: (1) filamentous primary hyphae in the first-invaded plant cell; (2) bulbous IH in first-invaded and in subsequently invaded plant cells; and (3) filamentous IH that initially grow in successively invaded cells (Table 2). Primary hyphae, first described by Heath et al. (1990), grew in lumens of first-invaded cells after pressure-based appressorial penetration (Howard and Valent, 1996; Talbot, 2003). Filamentous IH were produced in lumens of successively invaded rice cells after an internal wall penetration event that did not require high pressures (Figures 6F and 6G). Both primary hyphae and filamentous IH differentiated into bulbous IH. Primary hyphae resembled filamentous IH in diameter and in formation directly from highly constricted hyphal pegs that crossed the plant cell wall. Both primary hyphae and filamentous IH initially grew without nuclei, which must move across the hyphal pegs. Both were coated in plant membrane featuring distinctive membrane caps. On the other hand, primary hyphae differed from filamentous and bulbous IH in their accessibility to FM4-64 within the plant cell. That is, primary hyphae internalized FM4-64, whereas filamentous and bulbous IH did not. This finding suggested that primary hyphae differed from IH in their relationship to the host PM and their availability to the plant apoplast. Primary hyphae also differed from filamentous and bulbous IH in that they often lost viability after IH were established inside the host cell. Filamentous and bulbous IH remained viable as fungus spread to new rice cells in the developing lesion (Figure 7). These hyphal types, plus the more constricted penetration pegs and IH pegs that crossed the cell wall barriers, documented remarkable hyphal plasticity in the blast fungus as it successively colonized rice cells.

We clearly demonstrated that the specialized biotrophic IH of the rice blast fungus were sealed in a plant membrane, the EIHM, as they colonized living plant cells. Previously published discrepancies in the presence of a plant membrane surrounding blast IH may have been attributable to challenges in preserving membranes with conventional chemical fixatives used for TEM in these studies (Koga and Horino, 1984b; Heath et al., 1992). Even though the HPF/FS TEM used in our study is better for preserving membranes, artifactual breaks in membranes still occur (Bourett et al., 1999). Therefore, TEM images alone could not prove that the EIHM was continuous around IH, especially for extensive IH formed in the later stages of cell colonization. Our live-cell microscopy and FM4-64 dye-loading experiments provided a unique perspective on this issue (Figures 1, 3E, and 6E). The failure of IH to internalize FM4-64 suggested that the dye was not reaching the fungal PM because the fungus was sealed inside an EIHM that blocked passage of the dye. Interestingly, once IH developed, they were shielded from FM4-64 uptake even as they passed through cell walls. Thus, it appeared that the mechanism used by the fungus to cross plant cell walls maintained the integrity of the EIHM.

During plasmolysis, blast IH were always included within the shrinking plant protoplast, and the plant PM did not pull away from the IH wall (Table 1, Figures 3A and 3B). This finding suggests that there is a seal between the plant PM and the blast IH cell wall near the point where the hypha entered the PM, and/or that there is a tight connection between the EIHM and the IH wall. Inclusion of IH inside the plasmolyzing protoplast together with shielding of IH from apoplastically applied FM4-64 suggest that blast IH might be sealed inside the plant protoplast by a structure analogous to neckbands in biotrophic rusts and powdery mildews. Compared with other fungi that produce biotrophic intracellular hyphae, the relationship between blast IH and the rice PM during plasmolysis most closely resembled the relationship between intracellular hyphae of the monokaryotic parasitic stage of the cowpea rust fungus *U. vignae* and the cowpea PM (Heath et al., 1997). Events during plasmolysis in rice blast disease differed from plasmolysis events seen with the hemibiotrophic *Colletotrichum* species (O'Connell et al., 1985; O'Connell and Panstruga, 2006), in which the plant PM withdrew from biotrophic hyphae during plasmolysis.

We describe unique features of the blast EIHM. First, numerous FM4-64–stained connections were seen between the EIHM and rice membranes at the cell periphery (Figures 1I, 2C, 2D, and 6E). These EIHM–membrane connections were seen to change over time (Figures 2C and 2D). Second, prominent membrane caps were seen at the tips of primary hyphae and filamentous IH (Figures 3D and 3E). Membrane caps were no longer visible after these hyphae differentiated to bulbous IH. Similar structural features have not been described for other membranes encasing biotrophic intracellular hyphae or haustoria, and their roles have yet to be explored.

Although there is no uniform, organized interfacial matrix between the EIHM and the IH cell wall, localized elaborations containing electron-opaque, electron-transparent, and fibrillar materials were observed. Rare dramatic EIHM elaborations contained diverse cellular components, including endoplasmic reticulum–like membranes, against the fungal cell wall (Figure 2F). This was the case even though comparison of the RB and FM4-64 staining patterns in infected cells (Figures 1A, 1B, and 2E) showed that rice endoplasmic reticulum generally remained outside the tight-fitting EIHM. Our TEM images showing the patchy nature of the EIHM–IH interface are consistent with findings in previously reported studies of the blast fungus–plant cell interface. Koga and Horino, (1984b) presented micrographs of IH with associated fibrillar material similar to the endoplasmic reticulum–like membranes we report, although they did not see EIHM in these images. Heath et al. (1992) reported that the cell walls of intracellular blast hyphae were closely surrounded by invaginated plant PM, except for areas of localized elaborations or electron-opaque patches inside the membrane.

Our early dye-loading experiments with FM4-64 documented tubular and round vesicles proliferating near developing IH, suggesting that these are part of the endocytotic compartment of host cells (Figures 2A and 2B). Future studies will include determining whether endocytosis inhibitors block the formation of these plant vesicles. Inhibitors that specifically block plant and not fungal endocytosis would be most valuable for separating effects on the host from effects on the pathogen. Endocytotic vesicles might also be identified by immunolocalization of plant clathrin molecules with vesicles within invaded host cells (Stark-Urnau and Mendgen, 1995). The plant vesicular activity we report may function in nutrient uptake by the IH. Vesicular fusion would also provide a mechanism for the internalization of plant cell components within the EIHM (Figure 2F).

The mechanism for the origin of the EIHM, or of any plant membrane encasing biotrophic hyphal structures, is not known. It has generally been assumed that the plant membranes that surround biotrophic fungal structures are produced by invagination of the plant PM (O'Connell and Panstruga, 2006). Koh et al. (2005) showed that the EHM surrounding haustoria of the powdery mildew fungus in *Arabidopsis* was clearly differentiated from the PM by the absence of eight GFP-labeled PM proteins. They suggested two possibilities for the origin of the EHM: invagination of the PM with some mechanism for excluding normal PM proteins, and de novo membrane assembly by targeted vesicle trafficking. In the first scenario, lipids added to the PM by exocytosis around the cell periphery would allow increased PM capacity for invagination around growing haustoria. In the second scenario, lipids would be added directly to the EHM by specialized vesicular activity.

The extremely large surface area of EIHM that coats blast IH (Figures 1D and 6E), the extensive connections between the EIHM and peripheral rice membranes, and the curious membrane caps and inclusions raise the intriguing question of how the EIHM is constructed as IH grow. The large membrane surface area, especially around late-stage IH (Figure 6E), might suggest that de novo lipid biosynthesis is involved. However, reports in the literature that lipid biosynthesis inhibitors made the plant more susceptible to blast disease suggested that de novo lipid biosynthesis is not required for disease development (Koga, 1994b). Our working hypothesis is that the EIHM is being assembled de novo from redeployed plant membranes and that this assembly occurs by fusion of the dynamic plant membrane tubules and round vesicles around the expanding EIHM. We propose that the fungus redirects membrane trafficking in the plant cell to supply membrane components for building the EIHM.

Transgenic rice expressing fluorescent markers specifically labeling the plant PM and endocytotic compartments will provide important tools for understanding the source of the EIHM.

Knowledge that blast IH are wrapped in EIHM means that AVR-Pita and other rice blast effectors must be delivered across the EIHM to reach the rice cytoplasm. We recently showed that the fungus secretes the AVR-Pita avirulence protein (Orbach et al., 2000) into the membrane caps (Figures 3D and 3E) at the tips of both primary hyphae and filamentous IH (R. Berruyer, C.H. Khang, S.Y. Park, P. Kankanala, K. Czymmek, S. Kang, and B. Valent, unpublished results). The next step is to demonstrate the delivery of AVR-Pita protein across the EIHM into the rice cytoplasm. Studies of the delivery of fungal effectors into the host cytoplasm are in early stages for all fungal and oomycete systems. Demonstration of the secretion of a rust haustorial protein into the infected plant cell has been reported (Kemen et al., 2005), and a specialized secretion signal appears to play a role in the secretion of oomycete avirulence proteins into plant cells (Kamoun, 2006). Nothing is yet known of the fungal mechanisms for secretion inside living plant cells. Understanding these mechanisms is a critical area for future disease research.

Hemibiotrophy in the Rice Blast System

In this study of a highly aggressive pathogen in rice, sequentially invaded epidermal cells were initially alive, as determined by their ability to plasmolyze. All forms of IH were sealed in EIHM (Figures 1C to 1E, 3D, 3E, and 6E), and they underwent swelling and constriction (IH pegs) as they moved through internal cell walls. We did not observe the death of plant cells ahead of the growing front of the fungus, as would be expected for necrotrophic hyphae. Berruyer et al. (2006) used the EYFP-labeled strain KV1 to follow macroscopic lesion development in rice leaves, and they reported that the fungal growth front always preceded visible symptom development. We suggest that there is no distinct switch from biotrophy to necrotrophy for rice blast disease, at least in the highly compatible interaction we studied. From these findings, rice blast defines a novel paradigm for hemibiotrophic plant infection, one in which each successive plant cell invasion is biotrophic but individual invaded cells are no longer viable by the time the fungus moves into the next cell. We suggest that a defining feature of biotrophic invasion by the blast fungus is repeated movement through plasmodesmata into living host cells.

TEM analysis showed an apparent lack of damage at the sites where IH pegs crossed internal cell walls during biotrophic invasion (Figure 5D). This finding suggested that extensive enzymatic digestion of the plant cell wall is not involved in biotrophic invasion. Still, the blast fungus is capable of producing an array of plant cell wall–degrading enzymes, such as cellulases and xylanases (Dean et al., 2005), and cytological studies report extensive degradation of plant cell walls in heavily invaded tissue and at later time periods (Rodrigues et al., 2003). There are numerous reports that blast invasion involves extensive destruction of mesophyll cells (Heath et al., 1990; Rodrigues et al., 2003), suggesting that necrotrophic hyphae might play some role in colonization. Blast necrotrophic hyphae might produce cell wall–degrading enzymes for recovering remaining nutrients from plant cell walls in tissue that had already undergone biotrophic invasion. Defining exactly when

biotrophic hyphae switch to necrotrophic growth remains for future studies.

Although different strains of *M. oryzae* are specialized for specific grass species (Couch and Kohn, 2002), strains can be found that exhibit a continuum of symptoms on particular hosts. In nature, symptoms can range from no visible macroscopic symptoms, to larger brown necrotic spots that fail to sporulate, to sporulating lesions of different sizes (Heath et al., 1990; Valent et al., 1991). An extended biotrophic invasion strategy may be characteristic of the most susceptible interactions in the field. Perhaps less compatible interactions (resulting in smaller sporulating or nonsporulating lesions) featured in some studies involve a more necrotrophic growth strategy (Rodrigues et al., 2003; Zellerhoff et al., 2006).

Roles for Plasmodesmata during Biotrophic Blast Invasion

Although it is well known that viruses spread from cell to cell using plasmodesmata (Wolf et al., 1989; Oparka et al., 1997; Lazarowitz and Beachy, 1999; Zambryski and Crawford, 2000), the movement of an intact, relatively large eukaryotic organism like *M. oryzae* through plasmodesmata would require extraordinary constriction of the organism, significant plasticity in plasmodesmata, extensive modification of plasmodesmata, or a combination of these factors. However, several lines of evidence support our hypothesis that blast IH use plasmodesmata for their cell-to-cell movement: (1) blast IH searched for particular locations to cross the plant cell wall, and indeed, some IH apparently failed to find such suitable locations; (2) live-cell confocal imaging showed connections between EIHM and membranes at pit fields as well as extreme constriction of IH as they crossed the wall; and (3) HPF/FS TEM analyses found that IH preferentially contacted the plant cell wall at pit fields (Figures 5A to 5C) and documented IH crossing cell walls at pit fields (Figure 5D). Together, these results strongly suggested that IH search out plasmodesmata for crossing to the next cell.

Demonstration that the fungus did not move into guard cells from neighboring cells was highly suggestive that functional plasmodesmata are required for fungal cell-to-cell movement, because plasmodesmata degenerate as guard cells mature (Oparka and Roberts, 2001). However, the unique physiological properties of guard cells might make them unattractive for IH invasion. We found support in the literature that IH are able to grow inside a guard cell if it is penetrated by an appressorium (Heath et al., 1992; Koga, 1994a). Heath et al. (1992) described an infection site in which an appressorium had penetrated into a stomatal guard cell and formed a normal-appearing hypha that had grown to fill the cell. Koga (1994a) reported TEM analysis of the blast fungus invading rice panicle neck cells. That report includes a micrograph (Figure 4 in Koga, 1994a) showing an appressorium that had developed over the guard cells of a stomate. One of these guard cells contained an apparently healthy IH. Although it was not possible to confirm that this IH had entered the guard cell from the appressorium above it, this was likely to be the case. This image clearly shows that IH are capable of growing inside rice guard cells. Other micrographs from that report (Koga, 1994a) were consistent with our results in showing subsidiary cells that contained IH, but the IH had not moved into adjacent guard cells. From these combined studies, it appeared that IH were able to colonize guard cells through appressorial penetration but not by

moving from neighboring cells. Failure of IH to cross guard cell walls is consistent with the hypothesis that functional plasmodesmata are required for crossing internal cell walls.

Attempts to colocalize IH crossing the plant cell wall with plasmodesmata-specific markers have proven challenging. Plasmodesmata are commonly localized in plant cell walls by visualization of plasmodesmata-associated callose, which is involved in controlling the plasmodesmatal pore size in response to wounding (Lazarowitz and Beachy, 1999; Zambryski and Crawford, 2000). These studies involve either staining callose with aniline blue or immunolocalization with callose antibodies (Oparka and Roberts, 2001). We were unable to visualize plasmodesmata-associated callose with aniline blue because of the innate autofluorescence in the rice sheath cell walls (data not shown). The next step would be to use callose-specific antibodies to localize plasmodesmata. However, colocalization of callose and IH crossing plant walls may be ambiguous, because callose is a frequent component of collars, appositions, or extrahaustorial matrices surrounding fungal hyphae at cell wall penetration sites (Mims et al., 2004; O'Connell and Panstruga, 2006). Labeled plasmodesmatal proteins would provide a more specific probe for identifying plasmodesmata. Although pit fields in rice sheath cells were clearly labeled with fluorescently labeled TMV-MP using a microparticle bombardment transient expression assay, we were unable to find fungus growing in cells expressing TMV-MP. Future experiments will involve generating stable transgenic rice expressing fluorescent chimeric proteins that will label plasmodesmata in cells with growing IH.

There are literature reports that fungi move through pit pairs, pit field regions in plant tissues with thickened secondary walls. Koga (1994a) reported that the blast fungus invaded sclerenchyma cells of rice panicle neck tissue through pit pairs, where the cell wall is relatively thin because of a lack of secondary wall deposition. Two reports on cytological analyses of another pathogen, *Fusarium graminearum* infecting wheat spikes and stems, showed fungus moving into neighboring cells through pit pairs (Guenther and Trail, 2005; Jansen et al., 2005). *F. graminearum* is reported not to have a biotrophic stage (Jansen et al., 2005), and this fungus may have simply chosen the thinnest location to cross thick secondary cell walls. Nevertheless, these published reports suggest that fungi seek out and use pit fields for cell-to-cell movement, even though they do not mention the possibility that the fungus specifically uses plasmodesmata in these pit pairs.

Alternative mechanisms are possible if, indeed, the fungus is using plasmodesmata for its cell-to-cell movement. From the TEM analysis, we estimated that IH (>5 μm in diameter) were constricted at least 10-fold, to ~0.5 μm in diameter, at the point where they had crossed the cell wall (Figure 5D). One possibility is that IH use precisely controlled degradation of the pit field cell wall to produce a channel for their movement. The resulting channel should be large enough to accommodate the passage of an IH peg of this size. For this hypothesis, localized wall degradation would be facilitated by the unique structure of the plant cell wall in pit fields (Orfila and Knox, 2000). However, the appearance of an apparently normal plasmodesma next to crossing IH (Figure 5D) is inconsistent with the extensive degradation of pit field walls, because wall surrounding at least one plasmodesma survived during this crossing event.

Another possibility is that IH might manipulate individual plasmodesma to move into neighboring cells. From our TEM analysis, diameters of IH crossing the wall are at least 10-fold larger than diameters of plasmodesmata (30 to 50 nm). Thus, for an IH to fit through the plasmodesmatal channel would require further constriction of the initial IH peg beyond what we visualized and/or dilation of the plasmodesmatal channel. It is possible that the IH pegs that first penetrated the wall were thinner than the mature IH pegs seen in the TEM images and that they expanded the diameter of the opening after they passed through. It is known that appressorial penetration pegs are highly specialized for crossing physical plant barriers, because they initially lack normal cytoplasmic organelles and they contain abundant actin microfilaments (Bourett and Howard, 1992). After penetration, the cytoplasm, nucleus, and organelles of the fungus pass through the penetration peg into primary hyphae growing in the cell lumen (Howard and Valent, 1996). It is conceivable that IH pegs involved in crossing internal walls have a unique biological structure that facilitates their initial movement through plasmodesmata.

Neither hypothesis for how IH might be using pit fields/plasmodesmata has considered the complex components comprising functional plasmodesmata, including PM, desmotubule, protein, and cytoskeletal components. Our results show that the cell about to be entered is alive, with intact PM (plasmolyzes), and that the IH remains encased in EIHM. In Figure 6E, the EIHM appears continuous with a plant membrane that passed through the cell wall. These biological features make it less likely that the IH merely degrades pit field walls or empties the plasmodesmatal channel. Any mechanism that the fungus used to move through plasmodesmata would necessarily involve manipulation of the PM, endoplasmic reticulum, and proteins in these structures.

The blast biotrophic growth strategy in first-invaded cells clearly differed from its biotrophic strategy in subsequently invaded cells. Plant cells use plasmodesmata to communicate with each other when under abiotic or biotic stress (Lazarowitz and Beachy, 1999; Zambryski and Crawford, 2000). It is a reasonable prediction that the blast fungus might control plant signaling through plasmodesmata. The fungus might also prevent the invaded cell from alerting its neighbors by suppressing defenses in them. Biotrophic pathogens that produce haustoria are apoplastic. Hemibiotrophs such as *Colletotrichum* species have a biotrophic phase confined to one or a few host cells. The blast fungus differs from these biotrophs in its sequential intracellular biotrophic invasion strategy. Thus, the blast fungus might need to manipulate the plant processes it needs for biotrophic invasion in the host cells ahead of its growing front. Potential fungal control of plasmodesmatal signaling represents a novel area of plant disease research.

Understanding effector function requires the identification and functional analysis of candidate blast effectors. We have performed microarray analysis and identified genes that are only expressed by biotrophic IH in planta (G. Mosquera, S. Coughlan, and B. Valent, unpublished results). Proteins encoded by these genes are highly enriched for secreted proteins and therefore represent a rich source of blast effector candidates. Targeted gene disruptions are being used to identify functions for these putative effectors. We expect that rice blast effectors are involved in suppressing host defense responses, as has been shown in bacterial pathosystems (Desveaux et al., 2006). Blast effectors

may also redirect the plant membrane trafficking system for building the EIHM and for feeding. In addition, our research suggested novel biological functions for effectors in rice blast disease. We suggest that the fungus is manipulating the structure and function of plasmodesmata for its own cell-to-cell movement and for controlling plant cellular communication. As with studies of viral MPs (Wolf et al., 1989; Lazarowitz and Beachy, 1999), identifying fungal molecules that affect plasmodesmatal function may contribute to basic understanding of the structure and function of plasmodesmata in general and their role in plant signaling.

METHODS

Fungal Strains, DNA Manipulation, and Fungal Transformation

Magnaporthe oryzae strains O-137 (Orbach et al., 2000) and O-135 (Valent et al., 1991) were isolated from rice (*Oryza sativa*) in field plots at the China National Rice Research Institute in Hangzhou, Zhejiang, China, in 1985. Since collection, these field isolates have been stored dehydrated and frozen at −20°C such that they maintain full pathogenicity characteristic of aggressive field isolates (Valent et al., 1991). Guy11, a field isolate from rice in French Guiana, was obtained from J.L. Notteghem (Centre de Coopération Internationale en Recherche Agronomique pour le Développment). We generated strain KV1 by transformation of O-137 with pBV13 using a protoplast transformation protocol described previously (Sweigard et al., 1995). Plasmid pBV13 was produced by insertion of the *EYFP* gene from pEYFP (catalog No. 6004-1; BD Biosciences Clontech) into the *M. oryzae* vector pSM324 as described by Bourett et al. (2002). This vector contains a bialaphos resistance gene for selection and the constitutive promoter from the *M. oryzae* ribosomal protein 27 gene. The melanin biosynthesis mutant CP721 (*alb1-22*) contains a spontaneous mutation in the *ALB1* gene in field isolate O-135. To produce fungal strains with GFP-labeled nuclei, we transformed Guy11 with pAM1293 from Marc Orbach (University of Arizona). This plasmid was made by cloning the *ccg-1*-histone H1-GFP fragment from pMF280 (Freitag et al., 2004) and the hygromycin resistance gene from pCB1004 into pAM1145 (Kellner et al., 2005).

Infection and Plasmolysis Assays

Rice varieties YT-16 and Yashiro-mochi were grown as described (Berruyer et al., 2006). Leaf sheath assays have been used extensively for microscopy (Koga and Horino, 1984a; Koga et al., 2004). We used 3- to 4-week-old plants. Leaf sheaths from intermediate-aged leaves were cut into strips ~9 cm long. Fungal spores were harvested at a concentration of 10^5 spores/mL (unless noted otherwise) in 0.25% gelatin (type B from bovine skin; Sigma-Aldrich G-6650). Inoculum was introduced into the hollow space enclosed by the sides of the leaf sheaths above the mid vein. Inoculated sheaths were supported horizontally in a Petri dish containing wet filter paper such that the spores settled on the mid vein regions. When ready for microscopy, the sheaths were hand-trimmed to remove the sides and expose the epidermal layer above the mid vein. Lower mid vein cells were then removed to produce sections three to four cell layers thick. To observe plasmolysis, trimmed sheath tissue sections were mounted on microscope slides and observed directly in 0.75 M sucrose solution.

For infection with the *alb⁻* mutant CP721, the sides of the sheath were trimmed to expose the inner epidermal layer. This surface was wounded by rubbing 0.5-mm zirconia/silicon beads (catalog No. 11079105z; Biospec Products) on the inner sheath cuticle with a Q-tip. Spore inoculum was placed on the wounded surface. Fungus that grew on this tissue was reisolated to confirm that it still had the melanin-deficient phenotype.

Leaf drop inoculation assays were performed as described (Jia et al., 2003; Berruyer et al., 2006). Leaves from rice variety YT-16 were cut into 7- to 8-cm pieces and placed in Petri dishes with wet filter paper to maintain high humidity. Twenty-microliter droplets of spore inoculum at a concentration of 1×10^4 spores/mL were applied to the leaf pieces. Confocal imaging was performed at 75 hpi.

Microscopy

Confocal Microscopy

Hand-trimmed leaf sheath pieces were placed in a single-well Lab-Tek II chambered No. 1.5 cover glass system. Confocal images were acquired using a 63× C-Apochromat (numerical aperture 1.2) water-immersion objective lens on a Zeiss Axiovert 200M microscope equipped with a Zeiss LSM 510 META system. All spectral data for dual-labeled samples were collected with simultaneous 488-nm (EYFP) and 543-nm (FM4-64) excitation using 30-mW argon and 1-mW helium:neon lasers, respectively. Spectral scans were acquired using a 10.7-nm window from 510 to 610 nm. Reference spectra were acquired and used for linear unmixing to cleanly separate the overlapping EYFP and FM4-64 signals. Alternatively, samples labeled only with EYFP were imaged using 488-nm excitation with a 530-nm long-pass filter and DIC-transmitted light. In leaf assays, chloroplasts were visualized using 543-nm excitation with a 560-nm long-pass filter. All images are confocal except where mentioned otherwise.

DIC Microscopy

DIC imaging was done using a Zeiss Axioplan 2 IE Mot microscope. Cells were observed with a 63× C-Apochromat (numerical aperture 1.2) water-immersion objective lens. Images were acquired using a Zeiss AxioCam HRc camera and analyzed with Zeiss Axiovision digital image-processing software, version 3.1.

TEM

TEM was adapted from a published protocol (Bourett et al., 1999). Tissue discs were excised from infected sheaths at 24, 36, or 48 hpi using a 1.2-mm diameter biopsy punch, transferred to a 1-hexadecene–filled 1.2-mm to 400-μm HPF flat specimen carrier, and then frozen using a Leica EMPACT high-pressure freezer. Frozen samples were placed in a Leica EM AFS apparatus and freeze-substituted at −90°C for 3 d in 4% OsO₄ in acetone, warmed slowly to room temperature, rinsed three times in acetone, and embedded in Embed-812 resin. Sections were stained with lead citrate and uranyl acetate and imaged on a Zeiss CEM 902 transmission electron microscope equipped with a Megaview II digital camera (Soft Imaging System).

Tissue Staining Protocols

FM4-64 Staining

An aqueous 17 mM stock solution (Bolte et al., 2004) of FM4-64 (catalog No. 13320; Invitrogen) was made and stored at −20°C. Trimmed leaf sheaths and inoculated dialysis membranes were incubated in a 10 μM aqueous working solution for 30 to 120 min. Images in Figures 1B to 1E were stained differently. A stock solution was made at the concentration of 1 mg/mL in DMSO. Trimmed leaf sheath samples were incubated for 2 to 3 h in a working solution of 4 μg/mL in water.

Rhodamine B Staining

A stock solution of 10 μg/mL of the hexyl ester of rhodamine B (catalog No. R648MP; Invitrogen) was made in water and stored in 20-μL aliquots

at −20°C. Trimmed infected leaf sheaths were incubated in a 1 μg/mL working solution in 1× PBS for 30 min at 4°C, followed by 30 min at room temperature. The pieces were mounted in chambered slides with a drop of stain solution and imaged.

Propidium Iodide Staining

Propidium iodide was purchased as a solution of 1 mg/mL dye in water (catalog No. P3566; Invitrogen). An aqueous working solution of 100 μg/mL in 1× PBS was used to stain the tissues. Trimmed infected sheaths were incubated in dye solution for 15 min, followed by microscopy.

In Vitro Formation of Invasive-Like Hyphae

Conidia of strain KV1 were harvested from 10-d-old oatmeal agar cultures (Valent et al., 1991) in sterile distilled water and diluted to 1.0×10^5 spores/mL. Droplets of conidial suspensions were placed on 5- × 5-mm pieces of sterile, single-layered dialysis membrane in Petri dishes with moist filter papers. They were incubated at room temperature for 30 to 50 h (Bourett and Howard, 1990). Some dialysis membrane pieces were moved to 2YEG (2 g of yeast extract and 2 g of glucose per liter) nutrient agar plates after 35 h so that the invasive-like hyphae continued to grow.

Transient Expression in Rice

The gene encoding TMV-MP was amplified by PCR from vector pGreen0229, obtained from Karl Oparka at the University of Edinburgh. The gene was inserted into a pUC18-based vector that had been engineered for expression with the maize (*Zea mays*) ubiquitin promoter and an in-frame translational fusion to the sgfp-tyg (Heim et al., 1995) reporter gene. This construct was introduced into leaf sheaths with the aid of a particle inflow gun (Finer et al., 1992). Fifty milligrams of M10 tungsten particles (Sylvania) was suspended in 500 μL of water, and 25-μL aliquots were coated with 5 μL of DNA (2.4 μg/μL). Particles were vortexed, left at room temperature for 1 min, and mixed with 25 μL of 2.5 M $CaCl_2$ and 10 μL of 0.1 M spermidine. The particle suspension was vortexed and incubated on ice for 4 min, and 50 μL of the supernatant was discarded. The remaining mixture was vortexed. Leaf sheath tissues were placed in a Petri dish with wet filter papers and bombarded with 2 μL of the suspension at 60 p.s.i. pressure and 28 in Hg vacuum. This low pressure is important because high pressures in microprojectile bombardment experiments affect plasmodesmatal function (Zambryski and Crawford, 2000).

Supplemental Data

The following materials are available in the online version of this article.

Supplemental Movie 1. Multiple Membrane Tubules Were Visualized in an Invaded Epidermal Cell during Early Stages of FM4-64 Loading.

Supplemental Movie 2. Same Cell and Conditions as in Movie 1, but 4 min Later.

Supplemental Movie 3. Rice Membranes around the Developing IH after Loading to Saturation with FM4-64.

Supplemental Movie 4. Same Cell and Conditions as in Movie 3, but 90 min Later.

Supplemental Movie 5. IH Undergo Pseudohyphal Budding and Search for Locations to Cross Rice Walls.

Supplemental Figure 1. Extreme Constriction of IH Crossing Rice Cell Walls at 32 hpi.

Supplemental Figure 2. Swelling of IH Indicates Biotrophic Invasion in Rice Leaves at 75 hpi.

REFERENCES

Atkinson, H.A., Daniels, A., and Read, N.D. (2002). Live-cell imaging of endocytosis during conidial germination in the rice blast fungus, *Magnaporthe grisea.* Fungal Genet. Biol. **37:** 233–244.

Berruyer, R., Poussier, S., Kankanala, P., Mosquera, G., and Valent, B. (2006). Quantitative and qualitative influence of inoculation methods on *in planta* growth of rice blast fungus. Phytopathology **96:** 346–355.

Böhnert, H.U., Fudal, I., Dioh, W., Tharreau, D., Notteghem, J.-L., and Lebrun, M.-H. (2004). A putative polyketide synthase/peptide synthetase from *Magnaporthe grisea* signals pathogen attack to resistant rice. Plant Cell **16:** 2499–2513.

Bolte, S., Talbot, C., Boutte, Y., Catrice, O., Read, N.D., and Satiat-Jeunemaitre, B. (2004). FM-dyes as experimental probes for dissecting vesicle trafficking in living plant cells. J. Microsc. **214:** 159–173.

Bourett, T.M., Czymmek, K.J., and Howard, R.J. (1999). Ultrastructure of chloroplast protuberances in rice leaves preserved by high-pressure freezing. Planta **208:** 472–479.

Bourett, T.M., and Howard, R.J. (1990). *In vitro* development of penetration structures in the rice blast fungus *Magnaporthe grisea.* Can. J. Bot. **68:** 329–342.

Bourett, T.M., and Howard, R.J. (1992). Actin in penetration pegs of the fungal rice blast pathogen, *Magnaporthe grisea.* Protoplasma **168:** 20–26.

Bourett, T.M., Sweigard, J.A., Czymmek, K.J., Carroll, A., and Howard, R.J. (2002). Reef coral fluorescent proteins for visualizing fungal pathogens. Fungal Genet. Biol. **37:** 211–220.

Bryan, G.T., Wu, K., Farrall, L., Jia, Y., Hershey, H.P., McAdams, S.A., Faulk, K.N., Donaldson, G.K., Tarchini, R., and Valent, B. (2000). A single amino acid difference distinguishes resistant and susceptible alleles of the rice blast resistance gene *Pi-ta.* Plant Cell **12:** 2033–2045.

Cook, M.E., Graham, L.E., Botha, C.E.J., and Lavin, C.A. (1997). Comparative ultrastructure of plasmodesmata of Chara and selected Bryophytes: Toward an elucidation of the evolutionary origin of plant plasmodesmata. Am. J. Bot. **84:** 1169–1178.

Couch, B.C., and Kohn, L.M. (2002). A multilocus gene genealogy concordant with host preference indicates segregation of a new species, *Magnaporthe oryzae*, from *M. grisea.* Mycologia **94:** 683–693.

Czymmek, K.J., Bourett, T.M., Sweigard, J.A., Carroll, A., and Howard, R.J. (2002). Utility of cytoplasmic fluorescent proteins for live-cell imaging of *Magnaporthe grisea* in planta. Mycologia **94:** 280–289.

Dean, R.A., et al. (2005). The genome sequence of the rice blast fungus *Magnaporthe grisea.* Nature **434:** 980–986.

Desveaux, D., Singer, A.U., and Dangl, J.L. (2006). Type III effector proteins: Doppelgangers of bacterial virulence. Curr. Opin. Plant Biol. **9:** 376–382.

Farman, M.L. (2002). *Pyricularia grisea* isolates causing gray leaf spot on perennial ryegrass (*Lolium perenne*) in the United States: Relationship to *P. grisea* isolates from other host plants. Phytopathology **92:** 245–254.

Farman, M.L., Eto, Y., Nakao, T., Tosa, Y., Nakayashiki, H., Mayama, S., and Leong, S.A. (2002). Analysis of the structure of the *AVR-CO39* avirulence locus in virulent rice-infecting isolates of *Magnaporthe grisea.* Mol. Plant Microbe Interact. **15:** 6–16.

Finer, J.J., Vain, P., Jones, M.W., and McMullen, M.D. (1992). Development of the particle inflow gun for DNA delivery to plant cells. Plant Cell Rep. **11:** 323–328.

Freitag, M., Hickey, P.C., Raju, N.B., Selker, E.U., and Read, N.D. (2004). GFP as a tool to analyze the organization, dynamics and function of nuclei and microtubules in *Neurospora crassa.* Fungal Genet. Biol. **41:** 897–910.

Gancedo, J.M. (2001). Control of pseudohyphae formation in *Saccharomyces cerevisiae.* FEMS Microbiol. Rev. **25:** 107–123.

Genre, A., Chabaud, M., Timmers, T., Bonfante, P., and Barker, D.G. (2005). Arbuscular mycorrhizal fungi elicit a novel intracellular apparatus in *Medicago truncatula* root epidermal cells before infection. Plant Cell **17:** 3489–3499.

Guenther, J.C., and Trail, F. (2005). The development and differentiation of *Gibberella zeae* (anamorph: *Fusarium graminearum*) during colonization of wheat. Mycologia **97:** 229–237.

Harrison, M.J. (2005). Signalling in the arbuscular mycorrhizal symbiosis. Annu. Rev. Microbiol. **59:** 19–42.

Heath, M.C., Howard, R.J., Valent, B., and Chumley, F.G. (1992). Ultrastructural interactions of one strain of *Magnaporthe grisea* with goosegrass and weeping lovegrass. Can. J. Bot. **70:** 779–787.

Heath, M.C., Nimchuk, Z.L., and Xu, H. (1997). Plant nuclear migrations as indicators of critical interactions between resistant or susceptible cowpea epidermal cells and invasion hyphae of the cowpea rust fungus. New Phytol. **135:** 689–700.

Heath, M.C., and Skalamera, D. (1996). Cellular interactions between plants and biotrophic fungal parasites. In Advances in Botanical Research, J.A. Callow, ed (London: Academic Press), pp. 196–225.

Heath, M.C., Valent, B., Howard, R.J., and Chumley, F.G. (1990). Interactions of two strains of *Magnaporthe grisea* with rice, goosegrass, and weeping lovegrass. Can. J. Bot. **68:** 1627–1637.

Heim, R., Cubitt, A.B., and Tsien, R.Y. (1995). Improved green fluorescence. Nature **373:** 663–664.

Howard, R.J., and Valent, B. (1996). Breaking and entering: Host penetration by the fungal rice blast pathogen *Magnaporthe grisea.* Annu. Rev. Microbiol. **50:** 491–512.

International Rice Genome Sequencing Project (2005). The map-based sequence of the rice genome. Nature **436:** 793–800.

Jansen, C., von Wettstein, D., Schäfer, W., Kogel, K.-H., Felk, A., and Maier, F.J. (2005). Infection patterns in barley and wheat spikes inoculated with wild-type and trichodiene synthase gene disrupted *Fusarium graminearum.* Proc. Natl. Acad. Sci. USA **102:** 16892–16897.

Jia, Y., McAdams, S.A., Bryan, G.T., Hershey, H.P., and Valent, B. (2000). Direct interaction of resistance gene and avirulence gene products confers rice blast resistance. EMBO J. **19:** 4004–4014.

Jia, Y., Valent, B., and Lee, F.N. (2003). Determination of host responses to *Magnaporthe grisea* on detached rice leaves using a spot inoculation method. Plant Dis. **87:** 129–133.

Jia, Y., Wang, Z., Fjellstrom, R.G., Moldenhauer, K.A.K., Azam, M.A., Correll, J., Lee, F.N., Xia, Y., and Rutger, J.N. (2004). Rice *Pi-ta* gene confers resistance to the major pathotypes of the rice blast fungus in the United States. Phytopathology **94:** 296–301.

Kamoun, S. (2006). A catalogue of the effector secretome of plant pathogenic oomycetes. Annu. Rev. Phytopathol. **44:** 41–60.

Kawasaki, S., ed (2004). Proceedings of the 3rd International Rice Blast Conference. Rice Blast: Interaction with Rice and Control. (Dordrecht, The Netherlands: Kluwer Academic Publishers).

Kellner, E.M., Orsborn, K.I., Siegel, E.M., Mandel, M.A., Orbach, M.J., and Galgiani, J.N. (2005). *Coccidioides posadasii* contains a single 1,3-β-glucan synthase gene that appears to be essential for growth. Eukaryot. Cell **4:** 111–120.

Kemen, E., Kemen, A.C., Rafiqi, M., Hempel, U., Mendgen, K., Hahn, M., and Voegele, R.T. (2005). Identification of a protein from rust fungi transferred from haustoria into infected plant cells. Mol. Plant Microbe Interact. **18:** 1130–1139.

Koga, H. (1994a). Electron microscopy of early infection processes in the panicle neck of rice inoculated with *Pyricularia oryzae.* Ann. Phytopathol. Soc. Jpn. **60:** 89–98.

Koga, H. (1994b). Hypersensitive death, autofluorescence, and ultrastructural changes in cells of leaf sheaths of susceptible and resistant near-isogenic lines of rice (*Pi-z^t*) in relation to penetration and growth of *Pyricularia oryzae.* Can. J. Bot. **72:** 1463–1477.

Koga, H., Dohi, K., Nakayachi, O., and Mori, M. (2004). A novel inoculation method of *Magnaporthe grisea* for cytological observation of the infection process using intact leaf sheaths of rice plants. Physiol. Mol. Plant Pathol. **64:** 67–72.

Koga, H., and Horino, O. (1984a). Electron microscopical observation of rice leaves infected with *Pyricularia oryzae* Cav. in compatible and incompatible combinations. III. Resistance expression and loss of capability for plasmolysis in inner epidermal cells of leaf-sheath. Ann. Phytopathol. Soc. Jpn. **50:** 353–360.

Koga, H., and Horino, O. (1984b). Electron microscopical observation of rice leaves infected with *Pyricularia oryzae* Cav. in compatible and incompatible combinations. IV. The interface between invading hyphae and host cytoplasm in epidermal cells of leaf-sheath. Ann. Phytopathol. Soc. Jpn. **50:** 375–378.

Koh, S., Andre, A., Edwards, H., Ehrhardt, D., and Somerville, S. (2005). *Arabidopsis thaliana* subcellular responses to compatible *Erysiphe cichoracearum* infections. Plant J. **44:** 516–529.

Latunde-Dada, A.O. (2001). *Colletotrichum*: Tales of forcible entry, stealth, transient confinement and breakout. Mol. Plant Pathol. **2:** 187–198.

Lazarowitz, S.G., and Beachy, R.N. (1999). Viral movement proteins as probes for intracellular and intercellular trafficking in plants. Plant Cell **11:** 535–548.

Martinez, C., Roux, C., and Dargent, R. (1999). Biotrophic development of *Sporisorium reilianum* f. sp. *zeae* in vegetative shoot apex of maize. Phytopathology **89:** 247–253.

Mendgen, K., and Hahn, M. (2002). Plant infection and the establishment of fungal biotrophy. Trends Plant Sci. **17:** 352–356.

Mims, C.W., Richardson, E.A., Holt, B.F., III, and Dangl, J.L. (2004). Ultrastructure of the host-pathogen interface in *Arabidopsis thaliana* leaves infected by the downy mildew *Hyaloperonospora parasitica.* Can. J. Bot. **82:** 1001–1008.

O'Connell, R.J., Bailey, J.A., and Richmond, D.V. (1985). Cytology and physiology of infection of *Phaseolus vulgaris* by *Colletotrichum lindemethianum.* Physiol. Plant Pathol. **27:** 75–98.

O'Connell, R.J., Herbert, C., Sreenivasaprasad, S., Khatib, M., Esquerré-Tugayé, M.-T., and Dumas, B. (2004). A novel *Arabidopsis-Colletotrichum* pathosystem for the molecular dissection of plant-fungal interactions. Mol. Plant Microbe Interact. **17:** 272–282.

O'Connell, R.J., and Panstruga, R. (2006). Tête à tête inside a plant cell: Establishing compatibility between plants and biotrophic fungi and oomycetes. New Phytol. **171:** 699–718.

Oparka, K.J., Prior, D.A.M., Santa Cruz, S., Padgett, H.S., and Beachy, R.N. (1997). Gating of epidermal plasmodesmata is restricted to the leading edge of expanding infection sites of tobacco mosaic virus (TMV). Plant J. **12:** 781–789.

Oparka, K.J., and Roberts, A.G. (2001). Plasmodesmata. A not so open-and-shut case. Plant Physiol. **125:** 123–126.

Orbach, M.J., Farrall, L., Sweigard, J.A., Chumley, F.G., and Valent, B. (2000). The fungal avirulence gene *AVR-Pita* determines efficacy for the rice blast resistance gene *Pi-ta.* Plant Cell **12:** 2019–2032.

Orfila, C., and Knox, J.P. (2000). Spatial regulation of pectic polysaccharides in relation to pit fields in cell walls of tomato fruit pericarp. Plant Physiol. **122:** 775–781.

Peng, Y.-L., and Shishiyama, J. (1989). Timing of a cellular reaction in rice cultivars associated with differing degrees of resistance to *Pyricularia oryzae.* Can. J. Bot. **67:** 2704–2710.

Qu, S., Liu, G., Zhou, B., Bellizzi, M., Zeng, L., Dai, L., Han, B., and Wang, G.-L. (2006). The broad-spectrum blast resistance gene Pi9 encodes a nucleotide-binding site-leucine-rich repeat protein and is a member of a multigene family in rice. Genetics **172:** 1901–1914.

Rodrigues, F.A., Benhamou, N., Datnoff, L.E., Jones, J.B., and Belanger, R.R. (2003). Ultrastructural and cytological aspects of silicon-mediated rice blast resistance. Phytopathology **93:** 535–546.

Stark-Urnau, M., and Mendgen, K. (1995). Sequential deposition of plant glycoproteins and polysaccharides at the host-parasite interface of *Uromyces vignae* and *Vigna sinensis*: Evidence for endocytosis and secretion. Protoplasma **186:** 1–11.

Sweigard, J.A., Carroll, A.M., Kang, S., Farrall, L., Chumley, F.G., and Valent, B. (1995). Identification, cloning, and characterization of *PWL2*, a gene for host species specificity in the rice blast fungus. Plant Cell **7:** 1221–1233.

Talbot, N.J. (2003). On the trail of a cereal killer: Exploring the biology of *Magnaporthe grisea.* Annu. Rev. Microbiol. **57:** 177–202.

Urashima, A.S., Lavorent, N.A., Goulart, A.C.P., and Mehta, Y.R. (2004). Resistance spectra of wheat cultivars and virulence diversity of *Magnaporthe grisea* isolates in Brazil. Fitopatol. Bras. **29:** 511–518.

Valent, B., Farrall, L., and Chumley, F.G. (1991). *Magnaporthe grisea* genes for pathogenicity and virulence identified through a series of backcrosses. Genetics **127:** 87–101.

Ward, B.M., Medville, R., Lazarowitz, S.G., and Turgeon, R. (1997). The geminivirus BL1 movement protein is associated with endoplasmic reticulum-derived tubules in developing phloem cells. J. Virol. **71:** 3726–3733.

Wharton, P.S., Julian, A.M., and O'Connell, R.J. (2001). Ultrastructure of the infection of *Sorghum bicolor* by *Colletotrichum sublineolum.* Phytopathology **91:** 149–158.

Wolf, S., Deom, C.M., Beachy, R.N., and Lucas, W.J. (1989). Movement protein of tobacco mosaic virus modifies plasmodesmata size exclusion limit. Science **246:** 377–379.

Xu, H., and Mendgen, K. (1997). Targeted cell wall degradation at the penetration site of cowpea rust basidiosporelings. Mol. Plant Microbe Interact. **10:** 87–94.

Zambryski, P., and Crawford, K. (2000). Plasmodesmata: Gatekeepers for cell-to-cell transport of developmental signals in plants. Annu. Rev. Cell Dev. Biol. **16:** 393–421.

Zellerhoff, N., Jarosch, B., Groenewald, J.Z., Crous, P.W., and Schaffrath, U. (2006). Nonhost resistance of barley is successfully manifested against *Magnaporthe grisea* and a closely related *Pennisetum*-infecting linage but is overcome by *Magnaporthe oryzae.* Mol. Plant Microbe Interact. **19:** 1014–1102.